CellPress

Matter

Review

Skin-Interfaced Sensors in Digital Medicine: from Materials to Applications

Changhao Xu,[1] Yiran Yang,[1] and Wei Gao[1,*]

The recent advances in skin-interfaced wearable sensors have enabled tremendous potential toward personalized medicine and digital health. Compared with traditional healthcare, wearable sensors could perform continuous and non-invasive data collection from the human body and provide an insight into both fitness monitoring and medical diagnostics. In this review, we summarize the latest progress of skin-interfaced wearable sensors along with their integrated systems. We first introduce the strategies of materials selection and structure design that can be accommodated for intimate contact with human skin. Current development of physical and biochemical sensors is then classified and discussed with an emphasis on their sensing mechanisms. System-level integration including power supply, wireless communication, and data analysis are also briefly discussed. We conclude with an outlook of this field and identify the key challenges and opportunities for future wearable devices and systems.

INTRODUCTION

Skin is the largest organ of the human body. It protects the body as a physical barrier and harbors sophisticated sensations of touch and heat, enabling us to perceive temperature changes, pressure and vibrations, and texture and shapes of our surroundings. Mimicking the properties of human skin, wearable and flexible electronic devices provide an intimate yet non-invasive contact with the human body and are capable of digital monitoring of physical and biochemical signals. Compared with bulky, wired clinical equipment, these miniaturized on-skin sensors are characterized by real-time diagnosis and continuous monitoring, which open up new opportunities for long-term health assessment and disease diagnosis.

Over the past years, tremendous progress have been made in various aspects of wearable sensors including fundamental chemistries and materials,[1] mechanical engineering,[2] biological interfaces,[3] sensing techniques,[4] and non-invasive sensing demonstrations.[5] This review highlights the significant recent progress in wearable and flexible sensors, along with their applications in digital health assessment. In particular, we first summarize materials innovation and structural designs to manufacture flexible electronic materials that can be intimately attached to human skin; we then review flexible electronics for monitoring physical activities and physiological signals, such as body motion, skin temperature, heart rate, blood pressure, and pulse oximetry, as well as wearable chemical sensors for continuous molecular monitoring in biofluids including sweat and interstitial fluids. The systems-level device integration, including power supply, energy harvesting, wireless communication, and data transfer, is also briefly discussed. Finally, we discuss current bottlenecks and present our perspectives on potential future directions of this emerging field.

Progress and Potential

Skin-interfaced sensors present a great opportunity toward predictive analytics and real-time diagnosis in digital health. These wearable or mobile health (mHealth)-based electronic devices could not only monitor physical activities and vital signs but also keep track of molecular biomarkers of the human body. However, conventional wearable sensing systems and products face various challenges such as mechanical mismatch between the skin and rigid electronics during dynamic body motion, limited sensing functionality, signal extraction and physiological correlations of biomarkers, and long-term reliability. This review summarizes the latest advances of skin-interfaced wearable sensors, with an emphasis on materials, structural approaches, sensing strategies, and system configurations. Continued progress in this emerging field is promising for the development and commercialization of more reliable multifunctional wearable systems in the near future.

 © 2020 Elsevier Inc.

MATERIALS AND STRUCTURAL DESIGNS FOR SKIN-INTERFACED WEARABLE SENSORS

The integration of wearable sensors with the human body demands that the mechanical properties of the sensors should be soft, stretchable, and compliant to curved skin (Figure 1A). Silicon is the default material for semiconductor electronics, but its modulus is ~100,000-fold higher than that of the human skin. Considering the huge mechanical mismatch, the most intuitive approach is to develop intrinsically soft and conducting materials to achieve mechanical compatibility and improved wearing comfort. Several review articles have been published with emphases on materials synthesis, structural engineering, and platform designs.[2,6–11]

Soft Electronic Materials

Liquid Conductors

Liquid conductors, such as liquid metals and ionic liquids, have infinite stretchability while maintaining high conductivity due to their fluidic nature. Gallium metal alloys, particularly eutectic gallium indium (EGaIn) and Galinstan (GaInSn), are commonly used due to their low toxicity and negligible vapor pressure. Ga-based alloys will rapidly form an atomically thin oxide layer (Ga_2O_3) on their surfaces when exposed to ambient air, which holds the metal flush and enhances mechanical stability. Direct printing (e.g., three-dimensional [3D] printing) of complex structures of liquid metals has been realized at high resolution (Figure 1B).[12] In addition, ionic liquids, which are liquid salts at room temperature, can be combined with liquid metals to form liquid-state heterojunction sensors. These materials are typically embedded in fluidic channels of elastomers and exhibit superior conductivity even during stretching (Figure 1C).[13]

Hydrogels

Hydrogels are 3D networks of hydrophilic polymers, which have been widely applied as biomaterials owing to their mechanical similarity with tissues and biocompatibility. Conductive hydrogels can be obtained by mixing hydrogel networks with conductive materials (Figure 1D).[14] Traditional gel synthesis methods include physical crosslinking by entanglement and chemical crosslinking by covalent bonds.[20] Physically crosslinked hydrogels have lower mechanical stiffness but show good self-healing capability (Figure 1E),[15] while chemically bonded hydrogels can withstand severe deformation but cannot recover bonding or maintain conductivity after fracture.[21] Some recent manufacturing strategies involve double networks and sliding crosslinking to tailor to specific requirements of biomedical applications, tuning the Young's moduli from kilopascals to megapascals.[22–24] The major challenges of hydrogels are to realize robust bonding with other components and degradation due to water evaporation, which can be resolved by supramolecular chemical modification and elastomer encapsulation.[25]

Polymers

Intrinsically stretchable polymer materials represent another category of materials due to their well-studied chemical functionality and highly tunable properties. Conductive polymers are of particular interest due to their capability of interconnecting with other electronic components, including poly(2,3-dihydrothieno-1,4-dioxin)–poly(styrenesulfonate) (PEDOT:PSS),[16] poly(3-hexylthiophene) (P3HT),[17] polyaniline (PANI), polypyrrole (PPY), diketopyrrolopyrrole (DPP),[26] and their derivatives. As one of the most intensively investigated conductive polymers, PEDOT:PSS consists of conjugated PEDOT polymer doped by acidic PSS. Although both PEDOT and PSS are semicrystalline in nature with limited stretchability, coupling them with elastic substrates will improve their deformability greatly (Figure 1F).[16] One problem

[1]Andrew and Peggy Cherng Department of Medical Engineering, California Institute of Technology, Pasadena, CA 91125, USA

*Correspondence: weigao@caltech.edu

https://doi.org/10.1016/j.matt.2020.03.020

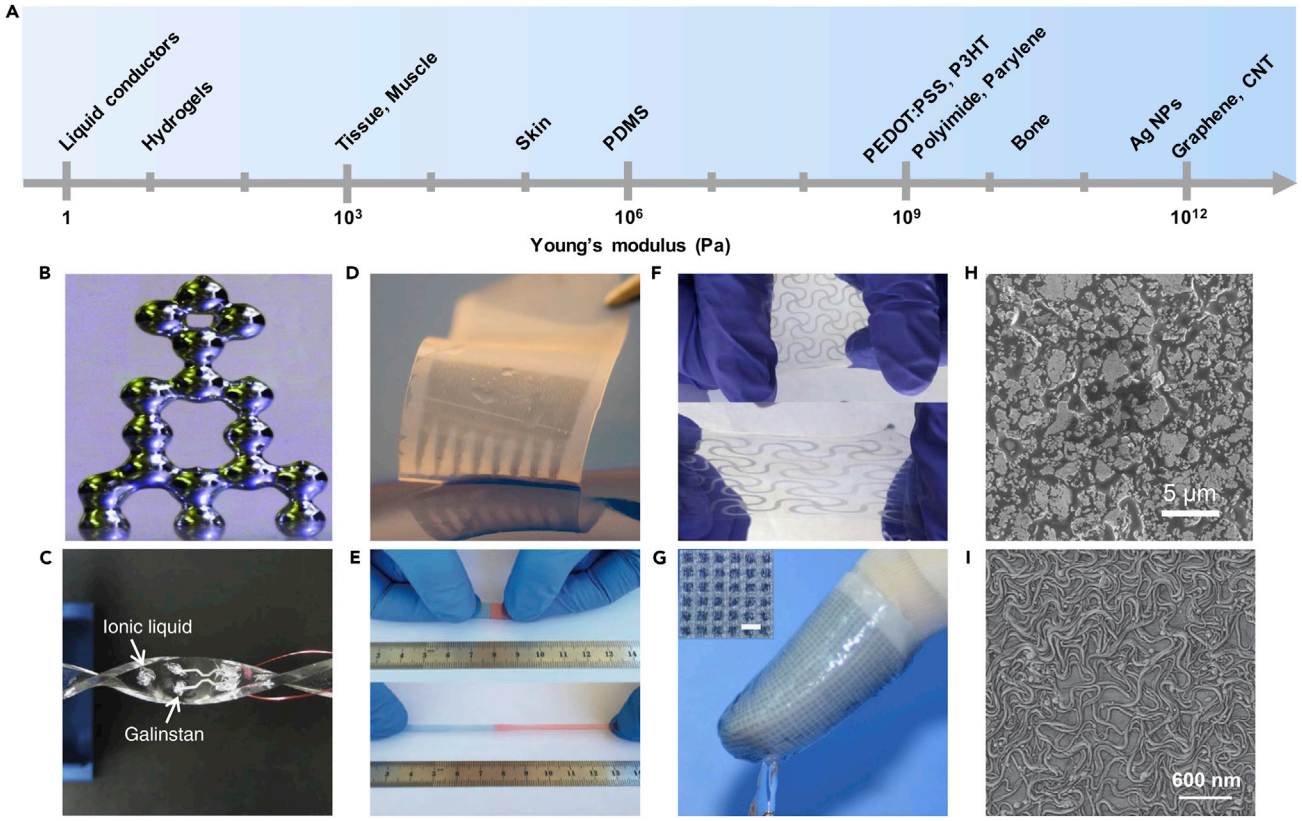

Figure 1. Soft Electronic Materials for Skin-Interfaced Wearable Sensors

(A) Comparison of Young's moduli among representative materials. NP, nanoparticles; CNT, carbon nanotubes.

(B) 3D-printed liquid metal arrays.

(C) A twisted liquid-state heterojunction sensor based on ionic liquid.

(D) A freestanding conductive hydrogel-based electrode array on soft jelly substrate.

(E) Self-healing hydrogel being stretched to five times its original length.

(F) A stretchable patterned PEDOT/STEC film on SEBS substrate.

(G) A semiconducting P3HT-based e-finger touching an ice cube.

(H) SEM images of elastic conductors formed of silver nanoparticles and flakes with surfactant.

(I) An AFM phase image of spray-coated carbon nanotubes on PDMS substrates.

Reprinted with permission from: (B) Ladd et al.[12] Copyright 2013, WILEY-VCH Verlag GmbH & Co. KGaA, Weinheim. (C) Ota et al.[13] Copyright 2014, Springer Nature. (D) Liu et al.[14] Copyright 2019, Springer Nature. (E) Cao et al.[15] Copyright 2017, WILEY-VCH Verlag GmbH & Co. KGaA, Weinheim. (F) Wang et al.[16] Copyright 2017, AAAS. (G) Zhang et al.[17] Copyright 2015, Springer Nature. (H) Matsuhisa et al.[18] Copyright 2017, Springer Nature. (I) Lipomi et al.[19] Copyright 2011, Springer Nature.

is that the polymer conductivity decreases with stretching, and ionic conductors are often added to overcome this issue. In addition to PEDOT:PSS, P3HT is another class of semiconducting polymer that can be utilized as the functional component for diodes and transistors (Figure 1G).[17] These semiconducting polymers along with their composites exhibit new functionalities of tunable conductivity and self-healability, and therefore are widely applied in developing all-organic stretchable electronic devices.[10,27]

Nanomaterials

Despite the rapid development in conducting polymers, most polymers are insulating or exhibit inherently low charge-transport efficiency, which often hinders their usage for interconnects of electronic components. Composite nanomaterials are therefore developed to combine conductive nanomaterial fillers and stretchable polymeric matrix.[28–31] Elastomers such as poly(dimethylsiloxane) (PDMS) and

Ecoflex are generally used as the matrix while nanomaterials of distinctive morphologies, classified as nanoparticles, nanowires, or nanosheets, are commonly adopted as fillers. For example, silver nanoparticles (AgNPs) can be mixed with fluorine rubbers and surfactant, where the fluorine rubbers have a strong polarity to metal ions and surfactant ensures homogeneous dispersion in this process. The fabricated printable elastic conductor exhibits potentials for large-area stretchable sensor networks (Figure 1H).[18] Higher electrical conductivity and smaller change in resistance under strain can be obtained using metal nanowires and carbon nanotubes (CNTs). For example, by uniformly dispersing CNTs in a solution, spray-deposited conducting thin films can be manufactured as electrodes in transparent sensor arrays (Figure 1I).[19]

The recent progress in materials science has enabled great opportunities for soft electronic materials for skin applications. However, there remain challenges for these developed materials. While liquid conductors such as gallium metal alloys have low toxicity and low activity and can provide infinite stretchability, most of these liquid conductors need microfluidic channels of carrying elastomer for skin sensors.[10,32] Hydrogels and polymers are highly biocompatible, but their performance is limited by their relatively low conductance, and many hydrogels suffer from drying out and stiffening over time. Current biocompatible materials are usually built with composite materials by combining hydrogels and polymers with nanomaterials to enhance their performance and stability. Caution should be exercised when using nanomaterials such as CNTs by encapsulating them inside elastomers to prevent potential health concerns.[33,34] Further development of biocompatible materials is desired for enhanced stability and breathability toward practical use.

Structure Engineering

Despite the progress in novel soft materials, conventional high-performance semiconductors are still indispensable in sensor data processing and transmission, yet these components are mainly built on rigid chips with metal interconnects. Structure engineering of electronic components provides a viable strategy to integrate silicon-based electronic components into wearable sensors. In addition, a curvilinear skin surface requires flexible structures with high mechanical stability to achieve intimate contact and reversible bending during daily motions and activities. Moreover, stretchable structures are needed to accommodate motion-related strain through controlled buckling. Here, we classify structure-engineered wearable devices based on different geometric designs, including ultrathin materials, wavy/wrinkles, serpentine, and mesh.

Ultrathin Materials

Considering that the bending strain decreases linearly with material thickness,[7] flexible electronics can be achieved simply by using ultrathin materials (Figures 2A and 2B).[35,36] An impressive example involves ultrathin plastic electronics with ultralight weight.[35] By building nanometers-thick organic transistors on an ultrathin polymer substrate, an imperceptible yet robust electronic foil could fold like a paper sheet and could be easily applied to curvilinear and dynamic surfaces. In addition, even rigid islands of chips can be wired out with thin metal wires as bridges. As shown in Figure 2C, an integrated pulse oximeter consisting of a rigid microcontroller and light-emitting diodes (LEDs) can be connected with thin copper wires and mounted on the human skin.[37]

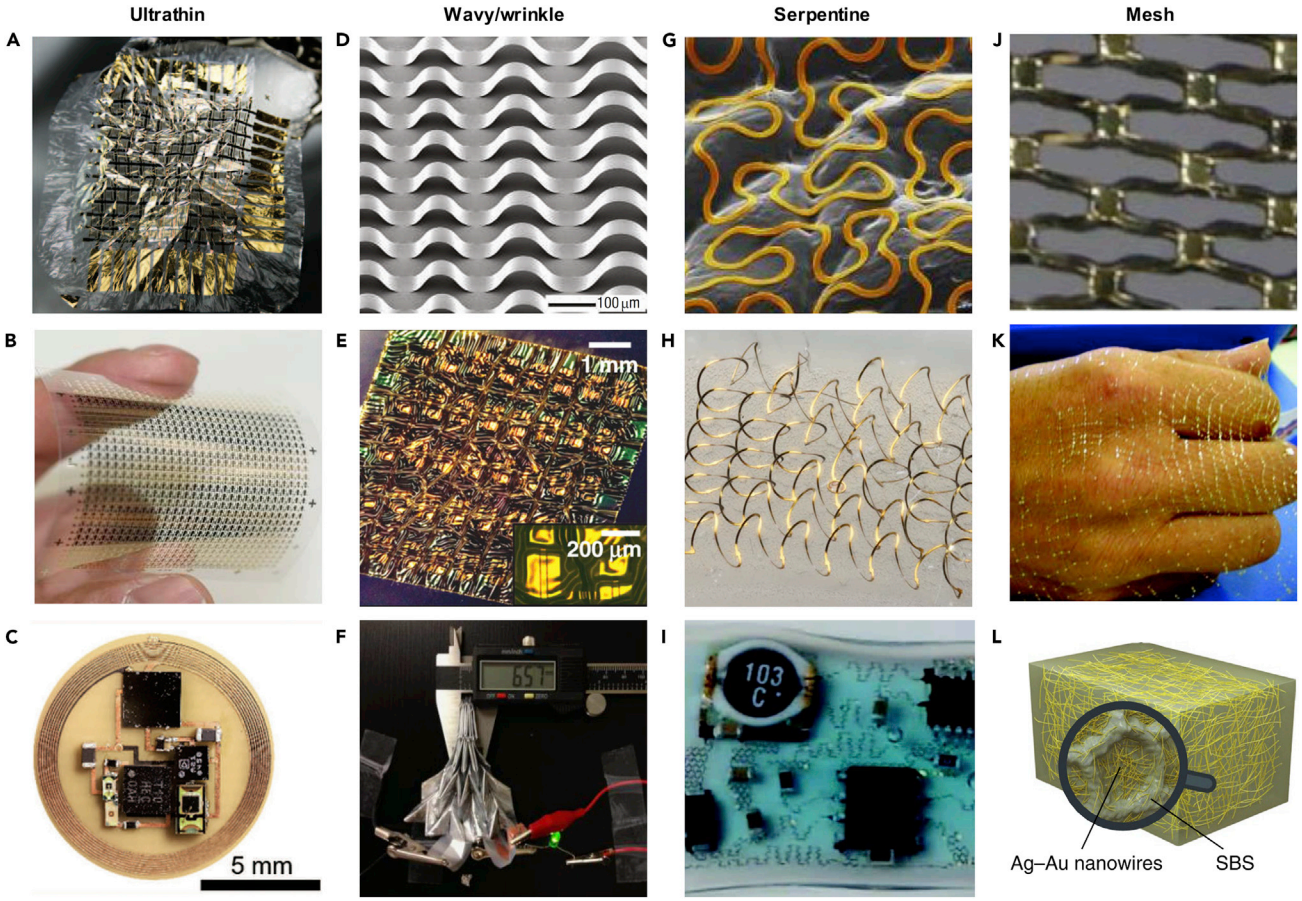

Figure 2. Structural Designs for Skin-Interfaced Wearable Sensors

(A) Paper-like ultrathin plastic electronic foils.
(B) Photograph of an organic memory cells array on a plastic substrate.
(C) Image of an NFC-enabled pulse oximeter.
(D) Controlled buckling of Si ribbons on elastomeric substrates.
(E) Stretchable and foldable CMOS circuit encapsulated in wrinkled PDMS.
(F) A compressed origami lithium-ion battery.
(G) Image of metal wires on skin replica.
(H) Image of a conductive helical coil network as interconnects for soft electronics.
(I) A stretchable electronic system that integrates rigid device circuits and a serpentine interconnect network in microfluidic suspensions.
(J) Image of a stretched pressure and thermal sensor network.
(K) A spider-web-like conductive network mounted on a hand.
(L) Schematic of microstructured Ag-Au nanocomposite in a soft matrix.
Reprinted with permission from: (A) Kaltenbrunner et al.[35] Copyright 2013, Springer Nature. (B) Sekitani et al.[36] Copyright 2009, AAAS. (C) Kim et al.[37] Copyright 2017, WILEY-VCH Verlag GmbH & Co. KGaA, Weinheim. (D) Sun et al.[38] Copyright 2006, Springer Nature. (E) Kim et al.[39] Copyright 2008, AAAS. (F) Song et al.[40] Copyright 2014, Springer Nature. (G) Fan et al.[41] Copyright 2014, Springer Nature. (H) Jang et al.[42] Copyright 2017, Springer Nature. (I) Xu et al.[43] Copyright 2014, AAAS. (J) Someya et al.[44] Copyright 2005, National Academy of Sciences. (K) Lanzara et al.[45] Copyright 2010, WILEY-VCH Verlag GmbH & Co. KGaA, Weinheim. (L) Choi et al.[46] Copyright 2018, Springer Nature.

Wavy and Wrinkled

To achieve not only flexibility but also stretchability, wavy and wrinkled layouts are introduced within the sensor platform, where structural deformations under applied external strains result in miniaturized strain inside the material itself. The fabrication method of these wavy structures is to bond planar devices to a uniaxially or biaxially pre-stretched elastomer with –OH groups on contacting surfaces, then release strain and drive the formation of wavy/wrinkle patterns through controlled buckling.[47] The compressive strain within the buckled device will offset the excessive strain when

applied to skin interfaces. The maximum stretchability of such a system depends on both pre-strain level and mechanical strength of solid materials. In the case of Si ribbons on PDMS (Figure 2D), the maximum stretchability is given by maximum pre-strain of 29%, plus 1.8% fracture strain and 0.034% critical strain of Si.[38,47] It is worth pointing out that this technique can be applied not only on ribbons and membranes but also on integrated circuit systems (Figure 2E).[39] Similarly, an origami technique introduces pre-defined hinge crease patterns to form a 3D structure, which could also fold and unfold without introducing much strain in functional components (Figure 2F).[40]

Serpentine

A serpentine design is a meandering structure that consists of periodically repeating geometric shapes (Figure 2G).[41] Optimizations of geometric parameters such as arc angle and width will produce skin-like moduli and bending stiffness. When applied to human epidermis, such structures provide electronic systems with conformal contact and similar mechanical properties. Given that serpentines can be either fully bonded to the substrate or selectively bonded with fixed local points, coils and helices represent 3D extensions of the 2D meandering serpentine structures, enhancing performances of both in-plane and out-of-plane stability against strain. A representative example assembles wireless, skin-compatible electronic sensors on the basis of 3D helical coils by deterministic compressive buckling of planar serpentine structures (Figure 2H).[42] Owing to their great compatibility with conventional flexible printed circuit board (FPCB) fabrication, the serpentine interconnections are intensively applied for sophisticated wearable sensor systems, as demonstrated in Figure 2I.[43] The serpentine features were suspended in soft microfluidics, together with isolated rigid sensors and circuits, to form a hybrid system laminated on skin.

Mesh

Mesh network is another structural layout that could achieve high stretchability. An early example demonstrates organic plastic film meshes of pressure and thermal sensors, with extended stretchability up to 25% (Figure 2J).[44] Higher stretchability of sensors can be established by adding serpentine layout to the meshes. Figure 2K demonstrates a spider-web-like sensor network based on a mesh of micronodes and extendible serpentine metal-coated polymer microwires. When external strain is applied, serpentine microwires will elongate to ten times their original length along with nearly undeformed nodes. The functional sensor network could undergo extreme strains up to 1,600% without damage or inducing microcracks.[45] Significantly, mesh networks can be obtained not only at macroscale but also within nanomesh structures. As shown in Figure 2L, gold-coated silver nanowires were combined within an elastomeric block-copolymer matrix. A mesh microstructure was generated because of phase separation in the nanocomposite during solvent drying. The nanocomposites yielded an optimized elongation of 266% while maintaining high conductance owing to the high aspect ratio of nanowires.[46]

There are numerous structural designs that can obtain conformal skin contact, yet there exists a trade-off between conductivity and stretchability. Higher stretchability needs longer wire connections and more complex designs, which will increase resistance and fabrication requirement. Current fabrication approaches, such as prestretching elastomer followed by strain release, introduce mechanical strain during the process. Thin-film designs face the challenge of integrating functional electronic integrated circuits for sophisticated sensing analysis. Some latest fabrication

processes such as stamp printing have been carried out, and developing versatile fabrication techniques for arbitrary 3D surfaces will become the key.[48]

Skin-Electronics Interface of Wearable Sensors

The integration of wearable sensors with skin needs to consider not only stretchable and biocompatible materials but also intimate contact forms on human epidermis. In this section, we review and classify skin interfaces into three forms: tattoo-like, medical band, and textiles.

Tattoo

Characterized by conformal and almost imperceptible appearance, tattoo-like wearable sensors represent an emerging class of ideal device forms. Since intimate physical contact can be achieved, many vital signals including electrocardiogram (ECG), electromyogram (EMG), and electroencephalogram (EEG) can be accurately monitored via tattoo-like sensors, as demonstrated in Figure 3A.[49] Additionally, chemical sensing can also be obtained in this form. In a representative application, tattoo-based non-invasive lactate monitoring was demonstrated through analyzing sweat during cycling exercise using an enzymatic biosensor (Figure 3B).[50] To enhance gas permeability and wearing comfort, a lightweight and breathable form of on-skin electronics was introduced, which laminated tattoo-like conductive nanomesh directly onto human skin (Figure 3C).[51] Long-term study of tactile sensing was shown without causing inflammation.[51]

Band

Sophisticated sensor systems, including rigid components such as integrated circuit chips, require alternative methods for on-skin applications. Medical bands are often used as a form of direct contact with skin without much discomfort. A polymer transistor-based pulse sensor can be simply mounted on skin using a commercial bandage to continuously monitor the pulse wave of the radial artery (Figure 3D).[52] Recently, a fully integrated wristband was developed with a chemical sensor array and FPCB for *in situ* analysis of sweat metabolites and electrolytes (Figure 3E).[53] Similarly, *in vivo* continuous monitoring of glucose levels in the interstitial fluid was achieved via a graphene-based band platform fixed onto the forearm (Figure 3F).[54]

Textile

Wearable textile sensors can be worn or knitted into fabrics for long-term continuous wear. Functional electronic components, such as antennas, resonators, and pressure sensors, can be fabricated from conductive textiles.[55,56] Such sensor fabrics can be designed as clothes or gloves for skin interfaces (Figures 3G and 3H). Notably, due to frictions with human body, textile wearable systems are generally utilized as an ideal platform for energy-harvesting applications. As shown in Figure 3I, a triboelectric energy generator (TENG) and supercapacitors were merged into clothes.[57] Through a natural arm-swinging motion during walking, energy harvesting and storage were demonstrated.

The key objective with skin interfaces is to achieve an intimate skin contact and collect high-quality sensing data. Rigid electronics induces gaps between devices and skin, which will generate artifacts and noise during motion. Meanwhile, many tattoo-based sensors still need to connect with external power supply and analysis instruments, and more studies involving low power consumption and fully stretchable skin electronics are being carried out.[58–60]

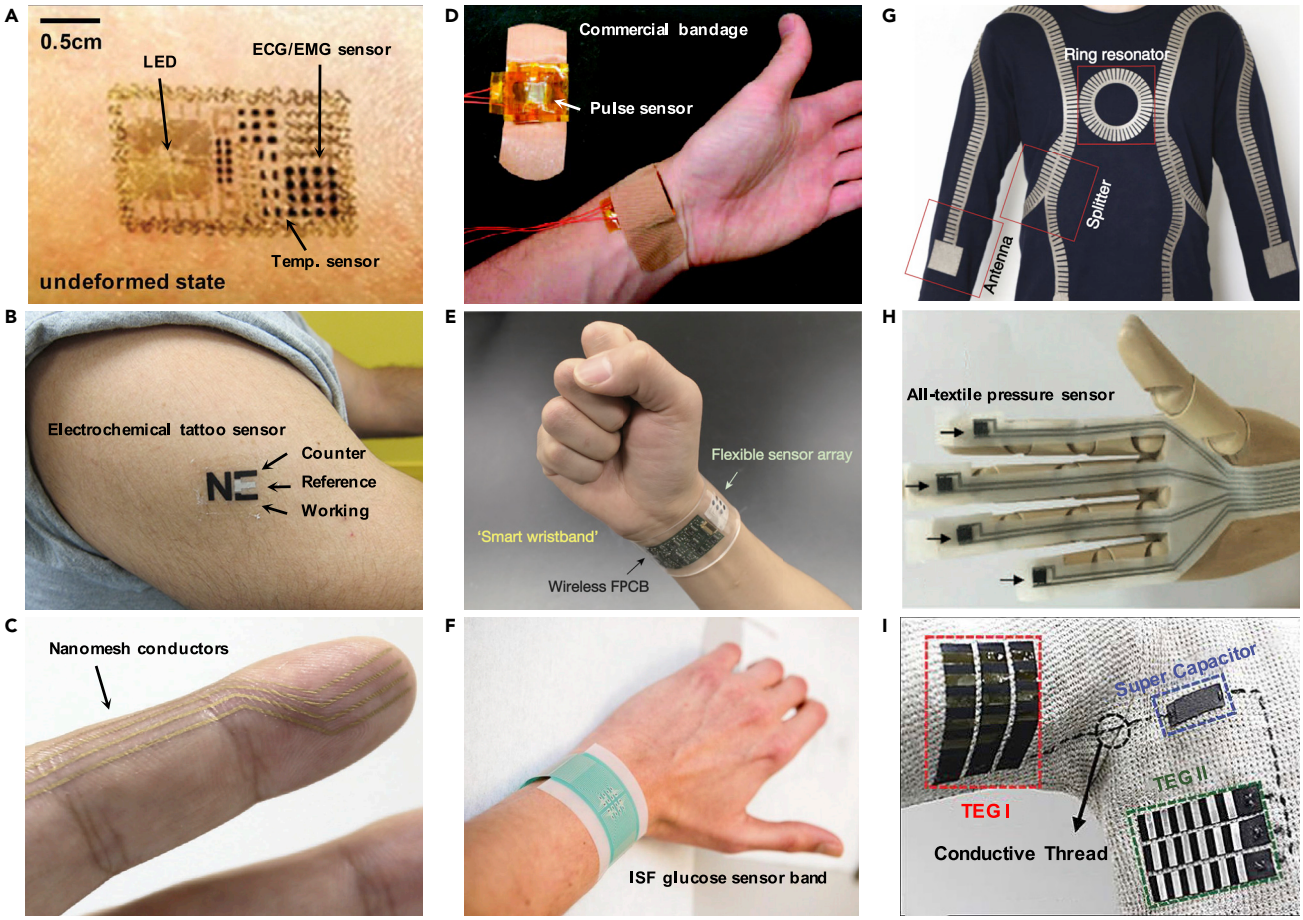

Figure 3. Skin-Electronics Interface of Wearable Sensors

(A) Tattoo-like epidermal ECG/EMG electronic system on skin.

(B) A lactate tattoo sensor applied to human skin.

(C) Photograph of gas-permeable nanomesh conductors attached to a fingertip.

(D) A pressure sensor measuring radial artery attached to the human wrist using an adhesive bandage.

(E) A flexible fully integrated wearable sensor array wristband for multiplexed *in situ* sweat analysis.

(F) Photograph of a graphene-based glucose-monitoring band on a subject's forearm for interstitial fluid (ISF) analysis.

(G) Image of a metamaterial textile sensor network for wireless communication.

(H) Photograph of textile pressure sensors mounted on fingers of an artificial hand.

(I) Image of a fabric-based triboelectric generator (TEG) applied to a knit shirt for activity monitoring.

Reprinted with permission from: (A) Kim et al.[49] Copyright 2011, AAAS. (B) Jia et al.[50] Copyright 2013, American Chemical Society. (C) Miyamoto et al.[51] Copyright 2017, Springer Nature. (D) Schwartz et al.[52] Copyright 2013, Springer Nature. (E) Gao et al.[53] Copyright 2016, Springer Nature. (F) Lipani et al.[54] Copyright 2018, Springer Nature. (G) Tian et al.[55] Copyright 2019, Springer Nature. (H) Liu et al.[56] Copyright 2017, WILEY-VCH Verlag GmbH & Co. KGaA, Weinheim. (I) Jung et al.[57] Copyright 2014, WILEY-VCH Verlag GmbH & Co. KGaA, Weinheim.

Skin-Interfaced Physical and Vital Sensors

Long-term monitoring of physical activities and vital signs is important in assessing the physical and mental state of a human, which is difficult to achieve with conventional gel electrodes as they dry out over time. Advances in wearable medical sensors have given rise to monitoring real-time physiological signals continuously and non-invasively. In this section, we summarize and classify these sensors along with their respective sensing mechanisms.

Temperature Sensing

The human body temperature is typically stable around 36.5°C–37.5°C. Elevated body temperature is often an indication of bacterial infection or inflammatory

conditions, while decreased temperature can reflect reduced blood flow or even organ failure. Therefore, body temperature is an essential vital sign for physiological health. A temperature sensor is also a critical component for tactile sensing in robotics and prosthetics. Measuring body temperature can be realized through thermistors,[61] infrared (IR) thermography,[62] and colorimetric means.[63]

As demonstrated in Figure 4A, a 3D-printed device was mounted on the ear like a headphone, which contained a thermopile IR sensor, data-processing circuits, and a wireless module.[62] The thermopile consists of a thermistor and an IR sensor; the former detects environmental temperature while the IR sensor calibrates temperature difference between target and background. The device measures core body temperature from ear drum accurately, regardless of environmental alterations and daily activities (Figure 4B). In another example, pixelated colorimetric temperature sensor arrays using thermochromic liquid crystals were patterned on PDMS elastomer substrate.[63] Digital cameras and wireless transmission systems enabled precise calibration and real-time readout, with temperature precision of 50 mK and submillimeter spatial resolution (Figure 4C). Figure 4D shows a mapping image of thermal characteristics of the skin, indicating temperature distributions due to blood flow of artery and veins at the wrist.

In contrast to optical measurements requiring either relatively bulky IR thermometer or complex calibrations by camera, some recent studies exploit electrical behaviors of materials against temperature that can easily measure skin temperature directly. Temperature coefficient of resistance (TCR) is one of the main considerations for thermistors. For example, the resistance of gold showed a linear response over body temperature range, which makes it an ideal material for skin electronics. Figure 4E shows an ultrathin conformal Au-based temperature sensor for thermometry.[61] The skin-like sensor consists of serpentine gold wires with thin polyimide encapsulation, which placed the metal near neutral mechanical plane for strain reduction and acted as a protection against moisture. A temperature sensor array was fabricated and directly attached onto skin of a human wrist. A clear spatial mapping of a 4 × 4 sensor array is shown in Figure 4F, which matched well with the result of an IR camera.

One problem within TCR-based sensors is that they can be easily affected by mechanical strain, which is unfavorable for on-skin applications. To better circumvent strain dependence of resistance-based sensors, a transistor-based temperature circuit was recently introduced (Figure 4G).[64] Such a bending-insensitive temperature sensor is designed using static and dynamic differential readout approaches based on stretchable CNT thin-film transistors (TFTs) (Figure 4H). The circuit generated a stable electrical output without being affected by temperature cycling or the induced stain range of 0%–60% during bending (Figure 4I).

There are numerous materials that correspond differently to temperature change, and for skin electronics, the simplest method is to use thin-film metals with high TCR such as gold. Another approach is to use semiconducting materials, which enable improved sensitivity by integrating them into transistors. One challenge for skin-interfaced temperature sensors is that most sensors measure skin temperature rather than core body temperature. Skin temperature can be easily affected by the surrounding environment while core body temperature is stable within 1°C fluctuations.[65] More correlation studies should be carried out to accurately measure the core body temperature based on skin temperature information.

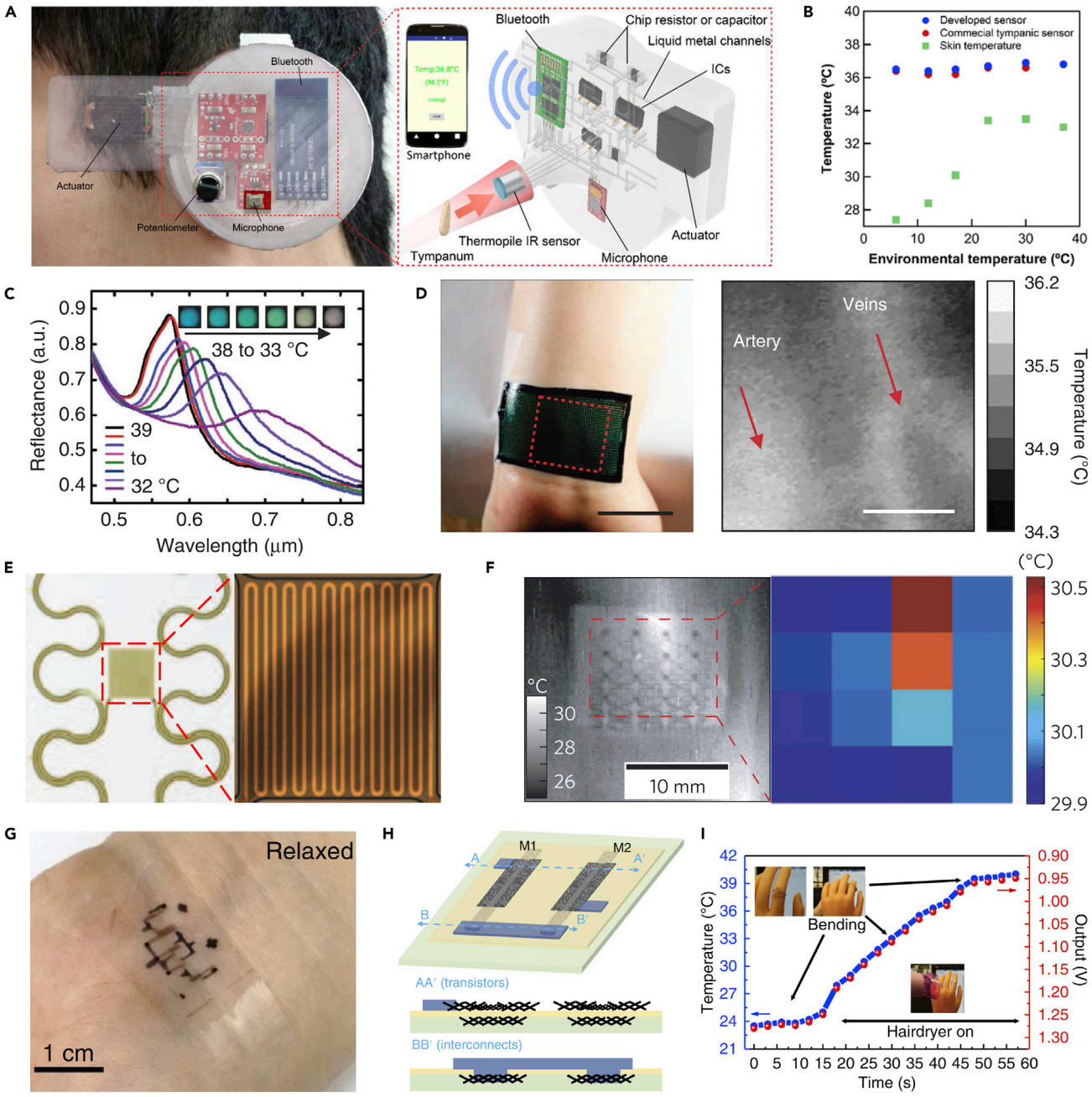

Figure 4. Temperature Sensing

(A) A core body temperature-detection system based on a thermopile IR sensor mounted on ear.

(B) Characterization of skin and core body temperatures as a function of environmental temperature.

(C) Calibration of reflectance of thermochromic liquid crystals (TLC).

(D) Optical image and infrared image of a colorimetric temperature sensor based on pixelated arrays of TLCs on the wrist.

(E) Image of a single temperature sensor based on temperature coefficient of resistance (TCR).

(F) Infrared image of a TCR device array mounted on the skin of the human wrist (left) and its corresponding temperature mapping (right).

(G) Image of an integrated circuit for strain-independent temperature sensing.

(H) Schematic of the structure of carbon nanotube (CNT) thin-film transistors (TFT) for circuits.

(I) Demonstration of stable functionality of temperature sensor attached to a prosthetic hand during repeated bending.

Reprinted with permission from: (A and B) Ota et al.[62] Copyright 2017, American Chemical Society. (C and D) Gao et al.[63] Copyright 2014, Springer Nature. (E and F) Webb et al.[61] Copyright 2013, Springer Nature. (G–I) Zhu et al.[64] Copyright 2018, Springer Nature.

Motion and Tactile Sensing

Tracing body motions and replicating skin sensory systems are crucial goals in the application of robotics and prosthetics. Wearable sensors are intensively applied in this field to continuously detect strain, pressure, vibrations, and deformations. Motion and tactile sensors, mainly in the form of pressure and strain sensors, can be realized through many transduction mechanisms, including piezoresistive, piezoelectric, capacitive, and triboelectric effects. Piezoresistive and capacitive sensors are most commonly used in skin-interfaced practices because of their simple designs and capability of acquiring both static and dynamic data.

Figure 5A presents an early example of a CNT strain sensor fixed to a glove.[66] The resistance-based strain sensor is composed of aligned single-walled carbon nanotube (SWCNT) film, which fractures into islands with bundles of CNTs connecting the gaps when stretched (Figure 5B). Such a design realized strain measurement up to 280%, 50-fold that of conventional metal strain gauges. By fixing multiple sensor sensors at the location of each knuckle on a glove, finger motions can be precisely detected and interpreted (Figure 5C).

Pressure sensing is the key component of tactile perception. Similarly, pressure sensors can also be realized through resistive or capacitive designs. For example, a strain sensor capable of pressure, shear, and torsion detection was designed using two interlocking layers of nanofibers.[70] The resistance of sensor changed dramatically according to the extent of interconnections under different stimuli, with excellent repeatability and reproducibility. However, most pressure sensors suffer from lack of ability to distinguish pressure from strain when mounted on skin, since these sensors are both achieved by deformation of structures, regardless of strain or normal pressure. To solve this issue, a groundbreaking study developed a strain-insensitive pressure sensor composed of composite nanofibers containing CNTs and graphene.[67] The key to this strategy is that fibers can change their relative alignment to accommodate deformation and reduce the strain in an individual fiber (Figure 5D). Through this approach, real-time pressure monitoring was demonstrated under different bending conditions, as shown in Figure 5E.

To mimic skin-like tactile sensation, pressure sensors need to be integrated as a large array to realize mapping of local forces. Thus, an intrinsically stretchable pressure sensory system with a device density of 347 transistors per square centimeter was developed.[58] The semiconductor was fabricated using a nano-confined fiber network to achieve high charge-carrier mobility. Since no rigid materials were used in the whole process, the transistor matrix could undergo 100% strain for 1,000 cycles without current-voltage hysteresis, seamlessly adhere to human skin, and allow spatial detection of extremely small local pressures, such as the landing of a bug (Figures 5F and 5G).

With the development of skin sensors that can independently detect motion, pressure, strain, temperature, and touch, engineering these sensors into a user-interactive human-machine interface has become a research focus. An early demonstration utilized organic light-emitting diodes (OLEDs) for pressure visualization by turning on diodes locally where the surface is touched (Figures 5H and 5I).[68] An array of 16 × 16 pixels was developed, whereby each pixel consists of an OLED, a pressure sensor, and an SWCNT transistor. The brightness of the OLED adjusts linearly with the magnitude of applied pressure as a result of conductance modulation of pressure sensor. More importantly, the user-interactive wearable sensors provide promising opportunities for skin prostheses. Figure 5J shows a prosthetic hand with a

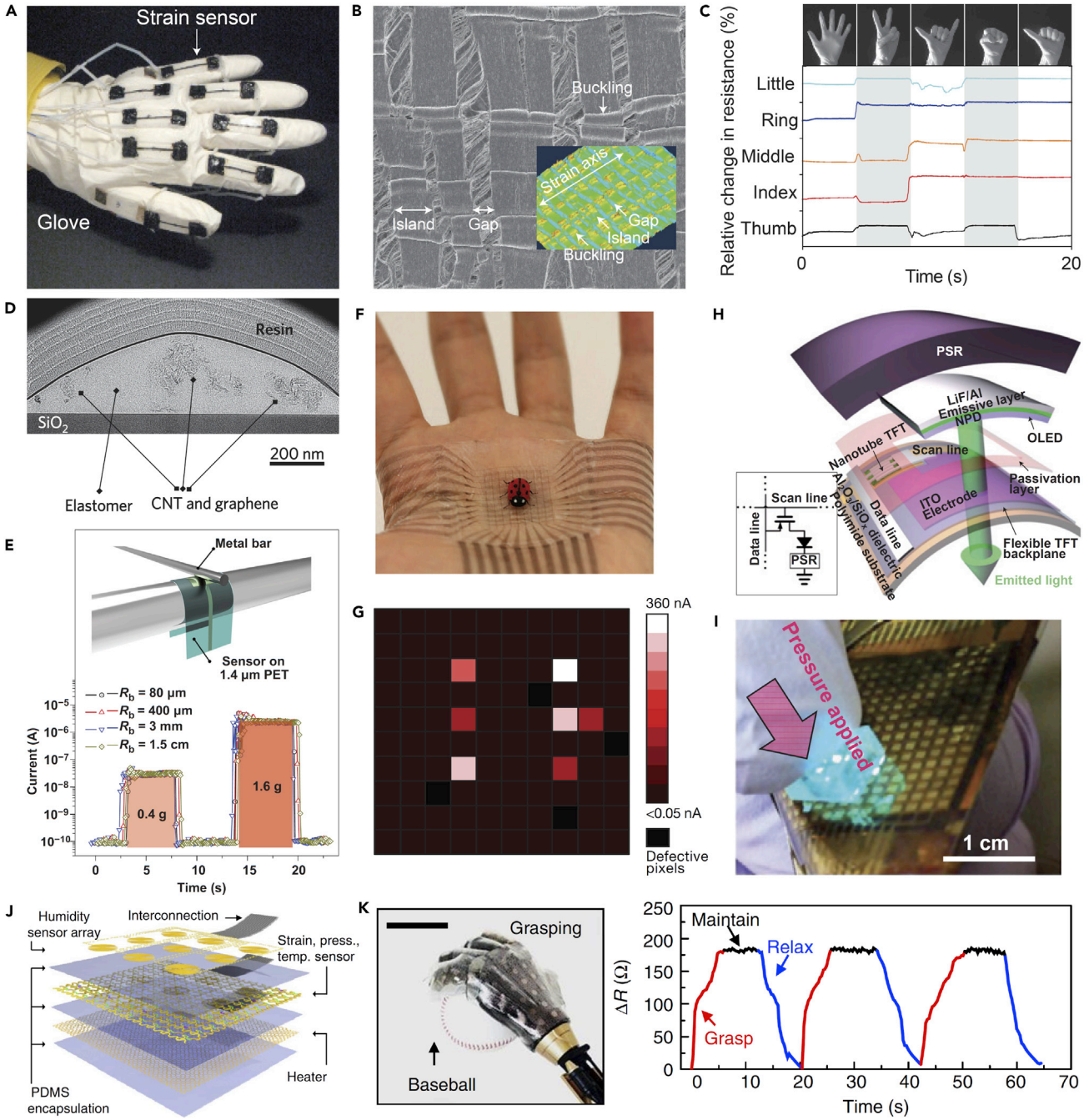

Figure 5. Motion and Tactile Sensing

(A) A CNT strain sensor array fixed to a data glove.

(B) SEM image of the fractural structure of the SWCNT film at 100% strain.

(C) Relative changes in resistance versus time for data glove motion of gestures.

(D) Cross-sectional HRTEM image of a single pressure-sensitive nanofiber.

(E) Performance of the pressure response of the device in various bending states.

(F and G) Current mapping of a stretchable transistor array (G), matching exactly with the position of a ladybug (F).

(H) Schematic of a single pixel of the user-interactive e-skin.

(I) Image of interactive e-skin device showing local light emission where the surface is touched.

(J) Exploded view of the artificial skin of a prosthetic hand.

Figure 5. *Continued*
(K) An image of the prosthetic limb catching a baseball, and the corresponding signal of the tactile sensor.
Reprinted with permission from: (A–C) Yamada et al.[66] Copyright 2011, Springer Nature. (D and E) Lee et al.[67] Copyright 2016, Springer Nature. (F and G) Wang et al.[58] Copyright 2018, Springer Nature. (H and I) Wang et al.[68] Copyright 2013, Springer Nature. (J and K) Kim et al.[69] Copyright 2014, Springer Nature.

laminated electronic skin integrated with strain, pressure, temperature, and humidity sensor arrays.[69] The system can accommodate complex daily operations such as grasping and manipulating objects, and temporal resistance readings of pressure sensors can be monitored simultaneously (Figure 5K).

Motion and tactile sensors are usually built with strain and pressure sensors based on either resistive or capacitive sensing. Most research uses networks of nanomaterials such as nanoparticles and nanowires, since these materials can be easily tuned for sensitivity by controlling density/sparsity. Another approach is to use 3D structures for higher sensitivity such as micropyramids, which harbor a wide application in vital sign monitoring and are mainly discussed in the following section.

Vascular Dynamics Monitoring

Biosignals including heart rate, pulse waveform, blood pressure, respiration rate, and pulse oxygenation are critical biomarkers of assessing cardiovascular health. In this section we discuss skin-interfaced wearable sensors that are capable of extracting this physiological information non-invasively and continuously.

Sensing the heart pulse electrically is similar to tactile sensation in that they are both based on pressure sensing. Resistive pressure sensors with high sensitivity and fast response time represent an early approach to collecting pulse signals. For example, an SWCNT film encapsulated with PDMS elastomer can show good sensitivity with a fast response time to detect pulse waveforms by loosely placing the sensor on the radial artery of wrist (Figures 6A and 6B).[71] The PDMS is patterned using a silk mold with crisscross structure, after which the SWCNTs can be exfoliated on microstructured PDMS substrate. This simple device was able to differentiate the subtle pulse wave distinction between a normal person and a pregnant woman (Figure 6C).

Capacitive pressure sensors represent another class of pulse-monitoring devices. Compared with resistance sensors, capacitors operate by capacitance or voltage change due to deformations of the compressible dielectric, which avoid direct current connection to the skin and thus enhance safety and stability. As shown in Figure 6D, a microstructured capacitive pressure sensor was placed on skin directly above the blood vessel.[72] The PDMS microhair structure consisting of periodic pillar arrays wrinkled and bent with skin deformation, which allowed conformal contact with irregular epidermis, while the micropyramids dielectric structure of the micropyramids enhanced pressure sensitivity. Signal amplification of about 12-fold was observed within the device, with a fast response and relaxation time (<10 ms) (Figure 6E).

Optical methods such as ultrasonic pressure sensors can also be used for pulse waveform observation. The ultrasound device can generate a penetration depth of around 4 cm deep into arterial and venous sites, and therefore is capable of monitoring deeply embedded central blood pressure waveforms at the neck (Figures 6F and 6G).[73] A pulse-echo method is applied to detect shifting echo frequency reflected from the anterior and posterior walls of the blood vessel. Figure 6H

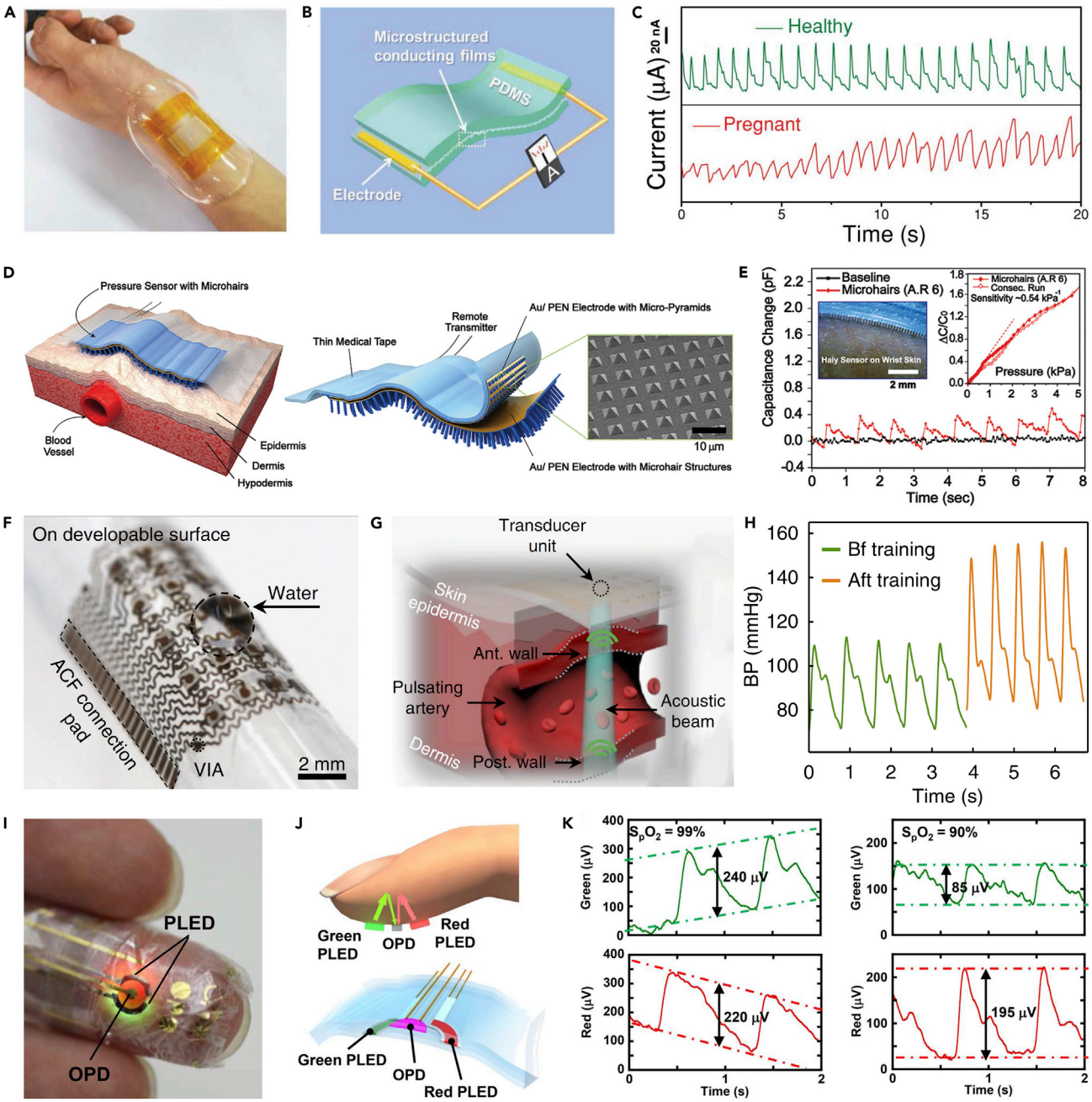

Figure 6. Vascular Dynamics Monitoring

(A) Photograph of a flexible resistive sensor for wrist pulse detection.
(B) Schematic of the pulse-sensing e-skin.
(C) Signals measuring wrist pulses of a healthy person and a pregnant woman.
(D) Schematic of a pressure sensor with microhair structures.
(E) Pulse waves of the radial artery measured with PDMS microhair sensors.
(F) A moisture-impermeable ultrasonic device conforming to complex surfaces.
(G) Sensing mechanism schematic of the pulse-echo method using an ultrasonic beam.
(H) Pulse waveform comparison measured before and after exercise.
(I) Photograph of an organic optical sensor mounted on a finger.
(J) Device structure and operation principle of the reflective pulse oximeter.

Figure 6. *Continued*
(K) Output signal from organic photodiode (OPD) with varying oxygenation of blood.
Reprinted with permission from: (A–C) Wang et al.[71] Copyright 2013, WILEY-VCH Verlag GmbH & Co. KGaA, Weinheim. (D and E) Pang et al.[72] Copyright 2015, WILEY-VCH Verlag GmbH & Co. KGaA, Weinheim. (F–H) Wang et al.[73] Copyright 2018, Springer Nature. (I–K) Yokota et al.[74] Copyright 2016, AAAS.

presents a pulse waveform before and after exercise measured by the ultrasound sensor after decoding, which shows clear arterial tonometry including systolic and diastolic pressure values. The measurement of vascular information also extracts pulse wave velocity, a significant parameter in arterial stiffness evaluation.

Alternatively, optical methods can be used to assess pulse oxygenation of a healthy adult. Non-invasive pulse oximetry measures peripheral oxygen saturation determined by oxyhemoglobin in the blood. As demonstrated in Figure 6I, an organic pulse oximeter consisting of polymer LEDs (PLEDs) and photodetectors were designed with pulse sensing and display on human skin.[74] The reflective pulse oximeter utilized a green LED and a red LED to generate two wavelengths of light through the finger, after which the photodetector at the same side as the LEDs measured the change in absorbance and determined peripheral oxygenation (Figure 6J). Typical photoplethysmogram signals of red and green LEDs are shown in Figure 6K, with varying oxygenation levels of blood.

Various methods, including electrical, ultrasound, and optical techniques, can be utilized to characterize vascular dynamics signals accurately, including pulse, blood pressure, and oximetry. Resistive sensors can be conveniently fabricated, but they often suffer from current drift and non-linear responses. Capacitive sensors are more prevalent in terms of stability and sensitivity. They can also be integrated into sensor arrays for spatiotemporal mapping. Compared with pulse and ultrasound sensing, optical measurement extracts signal of hemoglobin variations in blood, which does not require intimate skin contact and has been widely commercialized. One issue for these skin sensors is that the signals are highly vulnerable to motion artifacts. Signal-processing and noise-reduction techniques such as analog filters and amplifiers are required for daily applications.

Electrophysiology Monitoring

Electrophysiology studies involve electrical signals generated by biological cells and tissues. Common electrophysiological signals include ECG, EMG, EEG, and electrooculography (EOG). Soft, wearable skin sensors enable enhanced conformal contact along with great stretchability for dynamic daily operations on the skin.

ECG measurements are carried out by placing electrodes on the skin and detecting the electrical changes coming from heart muscle depolarization, which is a direct marker for cardiac diseases. Although conventional clinical ECG signals are carried out with 12 leads, the ECG extraction can be recorded by simply applying two electrodes on the chest. For example, conducting nanomaterials are often used as electrodes in a polymer network to fabricate stretchable ECG sensors.[75,76] However, fewer leads will also generate weaker signals and are more prone to noise interference. To improve signal amplification and stability without sacrificing conformity, amplifying circuit designs are often integrated with flexible substrates. Figure 7A shows a flexible organic differential amplifier for monitoring ECG signals, with functionalities of signal amplification and noise attenuation.[59] The amplifier was composed of organic TFT signal-processing circuit designs on a 1-μm-thick polymer foil, which also combined post-mismatch compensation to suppress the

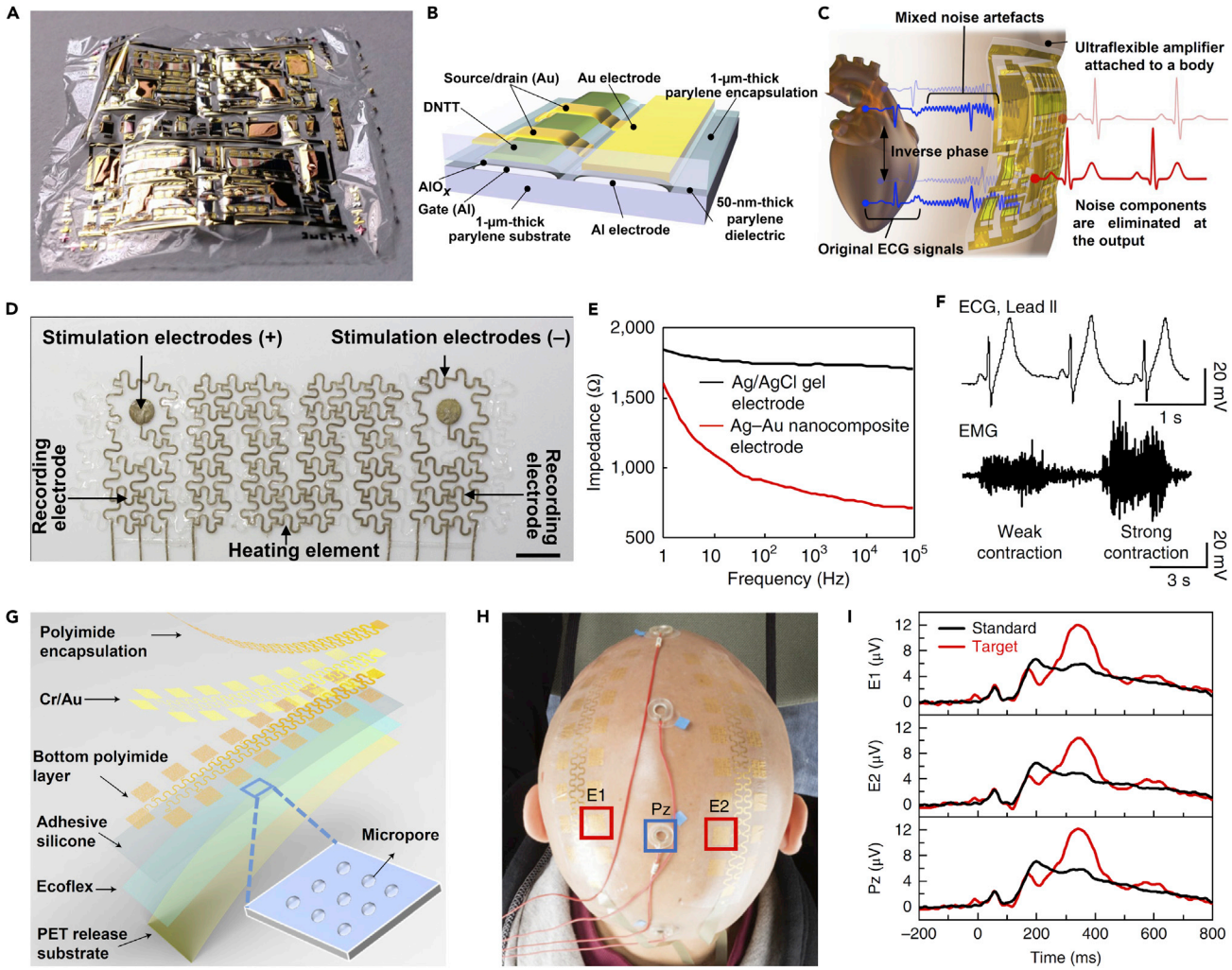

Figure 7. Electrophysiology Monitoring

(A) Image of an epidermal organic differential amplifier for electrocardiogram (ECG) monitoring.

(B) Cross-sectional schematic of organic TFT and thin-film capacitor in the circuit.

(C) Illustrations of ECG signal amplification and noise reduction based on differential amplifier.

(D) Image of an electrophysiological wearable electronic patch.

(E) Impedance comparison of the Ag-Au nanocomposite electrode and Ag/AgCl gel electrodes at the skin-electrode interface.

(F) ECG and electromyogram (EMG) recordings using the wearable device on the skin.

(G) Exploded view of the large-area epidermal electrodes for electroencephalogram (EEG) mapping.

(H and I) (H) Image comparison of epidermal (E1 and E2) and conventional EEG cup (Pz) electrodes on the scalp of a subject, and (I) corresponding recorded EEG signals.

Reprinted with permission from: (A–C) Sugiyama et al.[59] Copyright 2019, Springer Nature. (D–F) Choi et al.[46] Copyright 2018, Springer Nature. (G–I) Tian et al.[77] Copyright 2019, Springer Nature.

fabrication variations and ensure uniformity (Figure 7B). Enhanced signal-to-noise ratio performance was observed, with clear detection of the weak ECG signals even during human step motions (Figure 7C).

EMG collects the motor neuron signals to diagnose muscle and nerve conditions. The electrodes are attached to epidermis and measure the potential speed and amplitude between neighboring electrodes. For example, a wearable electronic patch was developed using Ag-Au nanowires in elastomer, with capabilities of ECG and EMG monitoring and stimulation electrodes (Figure 7D).[46] The Ag-Au

nanocomposite exhibited a high conductivity of 41,850 S cm^{-1}, which resulted in a lower contact impedance on the skin than that of conventional Ag/AgCl gel electrodes. This enabled concurrent detection of ECG and EMG with a high signal-to-noise ratio (Figures 7E and 7F). In addition, by placing EMG sensor patches at different epidermal locations, they can be used to monitor muscle disorders such as dysphagia.[78]

EOG measures potential variations between the inner and outer canthus, which is useful for monitoring eye movement and ophthalmological diagnosis. Different from other electrophysiological potentials, EOG measurements are usually carried out in DC potentials, which makes stable EOG signals challenging since DC recordings are susceptible to drift over time. In this circumstance, capacitance-based sensors are more favorable because the electrodes are fully encapsulated from surroundings. For example, a capacitive electronic system was developed using insulated electrodes for measurement, ground, and reference.[79] The performance of the capacitive sensor was quite similar to that of conventional direct contact electrodes, and could be used for long-term monitoring.

EEG is a powerful technique not only to evaluate brain activities and neural disorders but also to facilitate brain-machine interfaces that provide cognitive and prosthetic control. As shown in Figure 7G, a large-area epidermal electrode array covering the full scalp was developed to monitor the electrical activity across the brain.[77] The electrophysiological sensor was built on a removable polymer support with microporous silicone adhesives for breathable skin interface. The epidermal system was compatible with magnetic resonance imaging (MRI) and could measure EEG signals simultaneously during an MRI scan (Figures 7H and 7I), and realized control of a transhumeral prosthesis by patients.

By placing wearable sensors on different locations, whether on wrist or chest or scalp, various electrophysiological signals including ECG, EMG, EOG, and EEG can be monitored. These signals can not only evaluate health conditions of the subjects[80] but also be used for brain-machine interfaces and robotics control.[81] More clinical correlation studies and further understanding in neuroscience will bring more opportunities to this field in the near future.

SKIN-INTERFACED CHEMICAL SENSORS

Wearable and flexible chemical sensing has attracted academic and industrial attention for its potential to aid in or even replace conventional healthcare analytics. Compared with conventional analytics, wearable sensing could provide continuous and non-invasive data collection, without bulky equipment or trained professionals needed for the readout of the chemical analyses. Skin-interfaced chemical sensors, tailored for on-skin sampling and chemical analyses, primarily target two important biofluids, sweat and interstitial fluid (ISF); analytes in biofluids, sensing techniques, and applications in other biofluids can be found in previous reviews.[4,5,82–85]

Wearable Sweat Analysis

Sweat, a biofluid easily accessible without invasive procedure, contains a myriad of biomarkers indicative of athletic performance and personal health. To detect these biomarkers, electrochemical and optical detection methods were applied.

Electrochemical Sweat Sensor

As the most common wearable sensing strategy, electrochemical detection measures the target molecule concentration by measuring the electrical signals (such

as current, potential, or charge) generated at the electrode-solution interface. Using electrochemical detection, a fully integrated sweatband was developed for prolonged real-time multiplexed sensing of sweat metabolites, electrolytes, and skin temperature *in situ* (Figures 8A and 8B).[53] Ion-selective electrodes were used to detect sodium and potassium concentrations potentiometrically, and enzyme-based amperometric sensors were used to measure glucose and lactate levels with real-time calibration based on measured skin temperature. The polyethylene terephthalate-based biosensors and the silicon integrated circuits were consolidated on an FPCB for further signal processing and data transmission to a mobile phone, rendering a mechanically skin-conformal platform that enabled sensitive and stable sensor reading and complex electronic functionalities. Recently, an all-laser-engraved wearable sweat sensor platform was developed (Figure 8C).[86] With a CO_2 laser performing raster or vector scans on a polyimide sheet, graphene-based chemical and physical sensors were engraved with custom patterns. Low levels of uric acid (UA) and tyrosine were detected in human sweat through direct electrochemical oxidation on the laser-engraved graphene electrode. The CO_2 laser was also used to engrave microfluidic patterns to achieve efficient sweat sampling. The device was further used to investigate the use of sweat UA as a non-invasive alternative for gout management. During a purine supplementation study, sweat UA fluctuated in a pattern similar to serum UA (Figure 8D). High correlation between sweat and serum UA was observed in the pilot study involving both healthy subjects and gout patients. In addition to monitoring, therapy functionality was also added in a highly transparent and flexible graphene-based glucose patch (Figure 8E).[87] Au-doped graphene was used as the sweat glucose-sensing substrate to achieve transparency with great sensitivity, and a serpentine gold structure was layered beneath for enhanced stretchability and mechanical stability (Figure 8F). The patch could accurately measure the sweat glucose concentrations over a day, and the glucose concentration reflected the fluctuation of blood glucose (Figure 8G). The feedback therapy of the device is achieved with a graphene-Au mesh heater, a graphene-based temperature sensor, and bioresorbable drug-loaded microneedles coated with phase-change materials (PCM). At high glucose concentration, the heaters were triggered to function so that temperature reading increased past the threshold transition temperature. As temperature reached transition temperature, the PCM coating on the drug-loaded microneedles was melted and drug was released from the needles to blood, realizing the feedback therapy for glucose management.

Aside from exercise-induced sweat, sweat could be also generated by iontophoresis, a technique that uses an electrical current to deliver sweat-inducing (muscarinic) materials into epidermis that stimulate the secretion of sweat glands. The commercially available iontophoresis device (Macroduct) is bulky and fails to comply with wearable use, and a tattoo-based platform that integrates both iontophoresis and sensing was developed (Figures 8H and 8I).[88] The iontophoresis electrodes help to deliver pilocarpine (muscarinic agent) into the skin at the anode area, while a three-electrode system (counter, reference, and working electrode) is used to detect alcohol concentration. The system is connected with an FPCB for further data transmission. Further correlation study between blood sweat alcohol levels was performed using an iontophoretic microfluidic sensing device (Figures 8J and 8K).[89] Instead of using commercially available pilocarpine gels that are solely muscarinic, the device utilized carbachol, a muscarinic and nicotinic agent that can stimulate sudo-motor axon reflex (SAR) sweating, a sweating event that happens at sweat glands surrounding the stimulated area. By sampling the area not in contact with the stimulant, mixing between stimulated sweat and stimulant-contaminated sweat was avoided. Hex-wicked microfluidic channels were used to sample sweat from the SAR

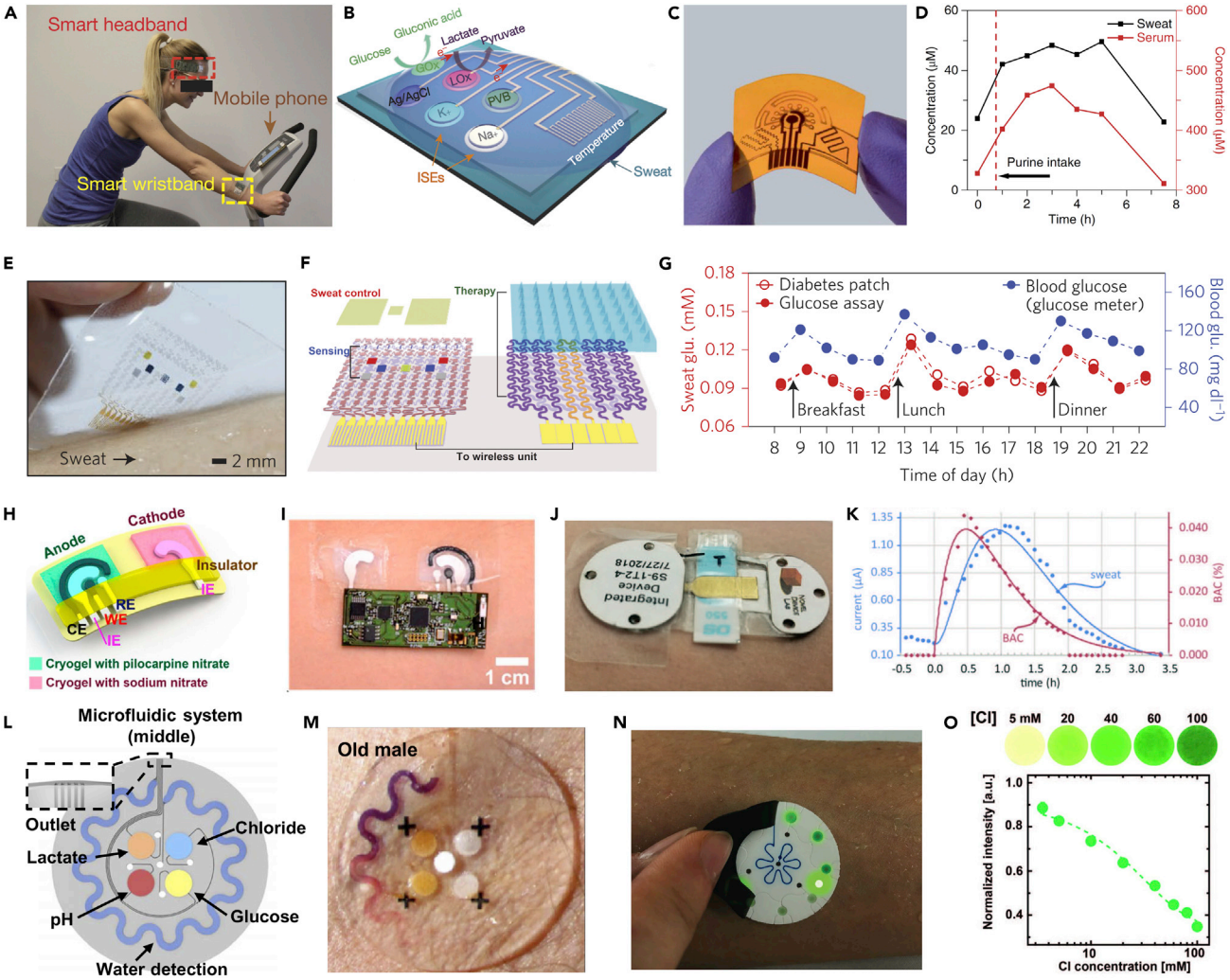

Figure 8. Sweat Analysis

(A) Fully integrated headband and wristband for on-body real-time perspiration analysis during exercise.

(B) Schematic of the sensor array for multi-analyte sensing.

(C) A laser-engraved sensor patch for sweat uric acid (UA) and tyrosine detection.

(D) Sweat and serum UA before and after purine intake on a healthy subject, measured by the laser-engraved sensor patch.

(E) Image of a graphene-hybrid electrochemical patch on the human skin.

(F) Schematic of the diabetes monitoring and therapy system.

(G) Sweat and blood glucose concentrations on a human subject over a day.

(H) Schematic of an iontophoretic device for alcohol sensing. IE, iontophoresis electrode; CE, counter electrode; RE, reference electrode; WE, working electrode.

(I) Photograph of the integrated tattoo device applied to a human subject.

(J) Photograph of an assembled device for blood-correlated sweat sensing.

(K) Pharmacokinetic curve of blood and sweat alcohol concentration.

(L) Schematic of colorimetric sensor patch for sweat lactate, glucose, creatinine, pH, and chloride ion determination.

(M) Sweat analysis during a cycling exercise.

(N) Photograph of a fluorometric sensor patch for sweat chloride, sodium, and zinc detection.

(O) Calibration plot of fluorescence intensity over chloride concentrations.

Reprinted with permission from: (A and B) Gao et al.[53] Copyright 2016, Springer Nature. (C and D) Yang et al.[86] Copyright 2020, Springer Nature. (E–G) Lee et al.[87] Copyright 2016, Springer Nature. (H and I) Kim et al.[88] Copyright 2016, American Chemical Society. (J and K) Hauke et al.[89] Copyright 2018, The Royal Society of Chemistry. (L and M) Koh et al.[90] Copyright 2016, AAAS. (N and O) Sekine et al.[91] Copyright 2018, The Royal Society of Chemistry.

sweating region to the alcohol-sensing screen-printed carbon electrodes. Using this device, a prolonged correlation (>3 h) between blood alcohol concentration and sensor measurements was achieved with a three-compartment pharmacokinetic absorption and elimination model.

Optical Sweat Sensor

Optical detection provides an attractive strategy for integrated chemical sensor measurements thanks to its cost-effectiveness and simplicity, utilizing optical transduction techniques such as colorimetric, fluorescence, and luminescence readout. Colorimetric sensors are widely used for wearable platforms, especially when incorporated with microfluidic systems. A soft and flexible microfluidic platform based on silicone elastomer was developed to detect lactate, chloride, glucose, pH, and sweat loss using colorimetric dyes (Figures 8L and 8M).[90] The dyes were spotted onto filter paper inserted in microreservoirs. The lactate and glucose measurements were achieved by incorporating enzymes with chromogenic reagents so that colorimetric readout was enabled. Near-field communication (NFC) was used to automatically launch the software on a mobile phone for image capture and analysis based on red-green-blue channel intensities. The system was validated during a prolonged cycling race and showed excellent adhesion stability and fluid-capture integrity. Another microfluidic-based fluorometric sensing platform was developed with a unique capillary-bursting valve design, which enabled chrono-sampling over time (Figures 8N and 8O).[91] As sweat fills one reservoir, the bursting valve opens due to pressure accumulation and enables sweat to go through downstream channels and enter the subsequent reservoir. After the fluorescent probes in the reservoir react with target analytes, the smartphone-based imaging module was applied for fluorescent imaging and analyses. Using this device, *in situ* chemical sensing of chloride, zinc, and sodium was achieved.

Recent advances in sweat sensing have revealed the potential of using sweat for non-invasive continuous health monitoring, as more clinically relevant biomarkers have been identified in sweat. However, there are still major challenges for continuous sweat monitoring *in situ*. One challenge is the efficient sweat sampling under low-sweat-rate conditions (i.e., sedentary individuals) in different sweat-stimulation scenarios. Minimized sweat sensors with high sensitivity should be used to accommodate small sample volumes. Another challenge is real-time calibration of chemical sensing. For some sweat analytes that are sweat rate dependent, the real-time measured concentration should be calibrated with sweat rates. In addition, secretion pathways of many newly discovered sweat biomarkers are yet to be understood or confirmed to achieve accurate calibration of the sensing results *in situ*.

Interstitial Fluid Analysis

ISF, present in most dermis and surrounding sweat and salivary glands, is an attractive source of rich biomarkers, since its analytes come from continuous capillaries and many analytes have almost similar concentrations between ISF and blood.[83] With this advantage, ISF has been investigated to detect various biomarkers, and various extraction methods have been created, such as sonophoresis and reverse iontophoresis.[92,93]

To extract ISF non-invasively, reverse iontophoresis (RI) was developed and integrated for ISF glucose detection on a tattoo interface (Figures 9A–9C).[94] The RI process involves applying a small current through the epidermis, causing the migration of cations to the cathode, leading to an electro-osmotic flow of ISF toward the cathode. The amperometric glucose-sensing electrodes were placed directly at the

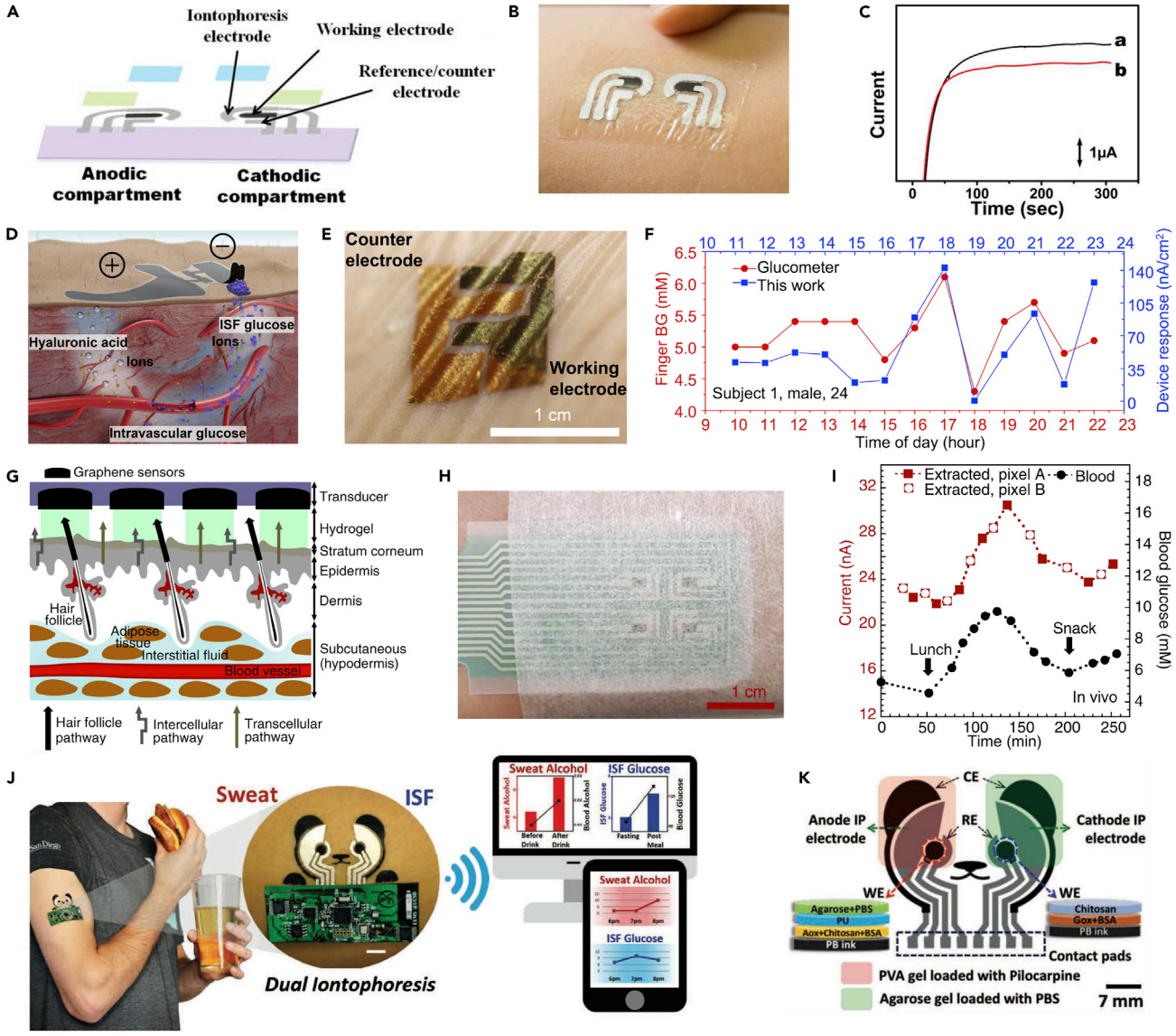

Figure 9. Interstitial Fluid Analysis

(A) Schematic of the tattoo sensor for non-invasive glucose sensing based on reverse iontophoresis (RI).
(B) Photograph of the tattoo-like sensing device on a human forearm.
(C) Amperograms of the tattoo-glucose sensor obtained pre- and post-meal from interstitial fluid analysis (ISF).
(D) ISF sensing mechanism by using RI with electrochemical twin channels (ETC).
(E) Image of RI electrodes attached to skin.
(F) Hourly glucose monitoring in comparison with a glucometer.
(G) Working principle of a glucose sensor array targeting transdermal individual preferential glucose pathways.
(H) Photograph of a screen-printed sensor array fixed onto a subject's forearm.
(I) *In vivo* continuous glucose monitoring on a healthy human subject using blood glucose as a reference.
(J) Demonstrations of a dual iontophoresis sensor for simultaneous sweat alcohol and ISF glucose detection.
(K) Schematic of electrode layout and composition of the working electrodes.
Reprinted with permission from: (A–C) Bandodkar et al.[94] Copyright 2014, American Chemical Society. (D–F) Chen et al.[95] Copyright 2017, AAAS. (G–I) Lipani et al.[54] Copyright 2018, Springer Nature. (J and K) Kim et al.[96] Copyright 2018, The Authors.

cathode region for direct measurement of ISF glucose and an increased post-meal current response was observed on human subjects, revealing the potential of ISF glucose for non-invasive diabetes management. To investigate the blood-ISF

glucose correlation, a system with electrochemical twin channels (ETC) and RI was developed (Figure 9D).[95] The ETC acted through high-density hyaluronic acid (HA), which was administered into the ISF under the anode. The extra HA increased the osmotic pressure of ISF and promoted blood glucose refiltration at arterial ends and reduced its reabsorption at venous ends, leading to a higher ISF glucose concentration, which in turn increased the RI flux. With increased glucose flux to supplement the as-is ISF glucose, better correlation could be established between the blood glucose and the extracted glucose in this ETC-RI procedure. The multilayered biosensors in the system included ultrathin layers of plastic substrate and nanostructured gold thin film, along with a nanoscale Prussian blue (PB) transducer layer and a glucose oxidase layer.[95] All the thin layers assembled rendered an ultrathin system that conformally laminates on the skin (Figure 9E) and enabled long-term monitoring of ISF glucose over a day, and the measured ISF glucose concentration correlated with blood glucose with remarkable consistency (Figure 9F). As most ISF glucose detection required finger-stick calibration, recent advances exploit a preferential glucose pathway (via hair follicles) to relax this calibration constraint. With a sufficiently dense pixel array and the correct pixel size, some of these pathways could be sampled randomly and individually by a pixelated device, which consists of pixelated ISF-sampling hydrogels containing glucose oxidase and in contact with graphene-Pt sensing electrodes (Figure 9G).[54] Integrating the sampling, sensing, and RI module into an elastomer platform, the device is flexible and easily laminates on human skin (Figure 9H). When tested on a healthy human subject, the two-pixel (operated in tandem) readout yielded solid agreement with the blood glucose level over 4 h, with an expected lag time of 15 min (Figure 9I). A dual iontophoresis system was developed to consolidate both sweat iontophoresis and ISF RI onto the same tattoo platform (Figures 9J and 9K).[96] The anode collected the induced sweat to measure sweat alcohol while the cathode sampled ISF for glucose detection. Both working electrodes were based on screen-printed PB ink as a transducer for the enzyme-based sensing. Agarose-containing phosphate-buffered saline was applied on top of the polyurethane to avoid pilocarpine interference on the PB electron-shuttling activity. The tattoo device was used for on-body amperometric sensing after meal and alcohol consumption, and displayed good correlation with a commercial blood glucometer and breath-analyzer devices.

Recent progress in ISF chemical sensing has opened tremendous opportunities for non-invasive skin-interfaced sensing, but some limitations are still to be resolved. The delay in ISF analyte response, either due to analyte diffusion time from the blood to the ISF or due to ISF extraction and collection time, could yield delayed detection of perilous conditions such as hyperglycemia or hypoglycemia. Continuous ISF extraction could still cause skin irritation. Smaller RI current and sporadic sampling could potentially alleviate the condition, but it is more desirable to discover more biocompatible and non-irritating methods for continuous ISF extraction.

Skin-interfaced chemical sensors show great promise for wearable health monitoring. The realization of their practical wearable application requires careful material selection in terms of detection sensitivity, stability, flexibility, and biocompatibility. For sweat and ISF sensing, many of the chemical targets could be difficult to detect due to ultralow concentration. The use of micro-/nanomaterial modification (e.g., CNTs, metal nanoparticles, graphene) could significantly increase the sensitivity, but the chemical stability of such modifications could deteriorate over time. Developing better techniques to immobilize the modification materials (i.e., Nafion) and applying anti-fouling materials (i.e., chitosan) could improve the stability of such chemical sensors toward continuous and long-term monitoring. In addition to

chemical stability, mechanical stability should also be of a concern. Thin and flexible sensor design not only helps to conform to skin curvature but also imposes less strain on the sensor during movements. Adhesion between sensor material and substrate is also crucial to prevent potential buckling events. The ideal chemical sensors should be strain resistant: incorporating a serpentine wire connection and reducing the active sensing area (while maintaining sufficient sensitivity) could also resolve strain-induced effects on sensor readings. The sampling process of sweat also requires flexible patches that conform and tightly adhere to skin to minimize sweat leakage. Many of the developed sweat sensors were directly placed in contact with the skin surface, which could cause contamination of the biofluids from the skin and local mixing of newly secreted and previously secreted sweat. Such a sampling scheme could induce errors and decrease temporal resolution in sensing results. Soft, thin microfluidics that route sweat from skin to an isolated sensor reservoir could be a good solution. In addition to efficient sampling, the use of microfluidics could prevent skin contact with the modified sensors and enhance the biocompatibility of the entire device. PDMS and thin medical adhesives are biocompatible and flexible candidates that could be used in direct contact with the skin.

TOWARD DIGITAL AND PERSONAL CONNECTED HEALTH

The full integration of miniaturized wearable sensors requires efficient power management and data-transfer techniques. Many skin-interfaced sensor systems have to compromise their functionality and stretchability due to the rigid and bulky batteries and electronic components. In this section, we review the recent development in energy supply and wireless data-transfer modules that are specially designed for wearable platforms toward digital and personalized healthcare.

Power

Flexible Batteries

Lithium-based batteries are the most commonly used energy storage devices, especially for applications with demanding power requirements, because of their high energy densities and excellent cycling performances.[97] Therefore, the flexible lithium-ion battery (LIB) is especially promising for multifunctional wearable applications. However, conventional LIBs contain flammable liquid electrolytes that can cause decomposition during bending and thus are poorly suited for flexible applications. To address this issue, solid-state electrolytes have been developed and many forms of flexible batteries have been introduced, including fibers, woven textiles, and polymer substrates. For example, an elastomer-encapsulated rechargeable LIB was demonstrated using polymer-based gel electrolytes (Figure 10A).[98] The flexible LIB was built by transfer printing of active materials and injecting gel electrolyte between $Li_4Ti_5O_{12}$ anodes and $LiCoO_2$ cathodes on a PDMS substrate, which could undergo 300% of strain. Inductive coils were also integrated into the stretchable device to enable contactless charging through external supplies. The silicone elastomer served as spacer between the sheets of electrode layers and as the encapsulation of the whole device. When mounted on the human elbow, the device is compliant to the curved elbow and able to light up a red LED (Figure 10B).

Solar Cells

Solar cells represent another promising energy supply by converting light energy through photovoltaic effect. For example, an ultraflexible self-powered electronic device was developed using organic photovoltaics as the power supply (Figures 10C and 10D).[99] The organic photovoltaics was patterned with nanograting morphologies on the charge-transporting layers, which increased power-conversion efficiency to 10.5% and achieved a high power-per-weight density of 11.46 W g^{-1}.

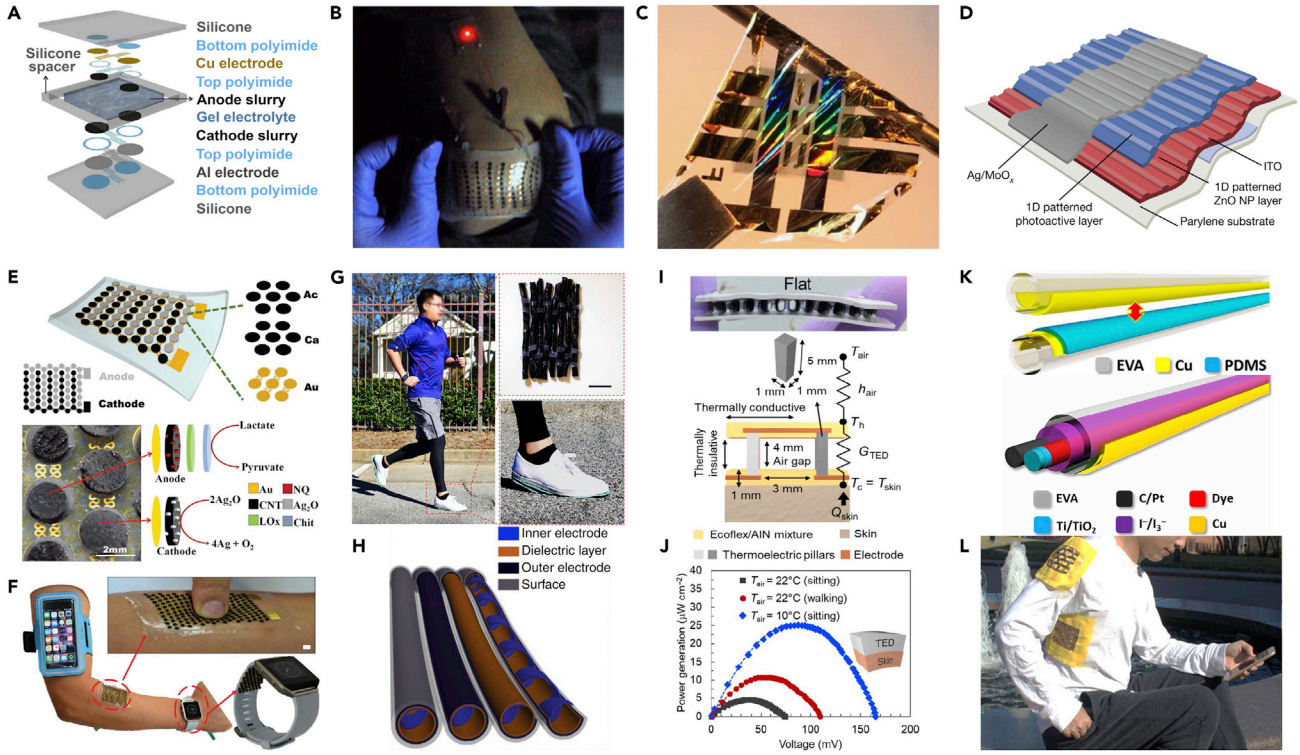

Figure 10. Power Supply

(A) Exploded view of a flexible lithium-ion battery.
(B) Image of the stretched battery mounted on the human elbow.
(C) Photograph of a flexible organic photovoltaics device wrapped over a rod.
(D) Schematic of the organic photovoltaics.
(E) Schematic of an e-skin-based biofuel cell and electrochemical reactions on electrodes.
(F) Demonstration of the BFC worn on a human subject.
(G) Demonstration of a triboelectric nanogenerator (TENG) assembled into clothes and shoes for power collection.
(H) Schematic of the tube-shaped TENG device.
(I) Photograph and schematic of a wearable thermoelectric device.
(J) Power generation of the thermoelectric device under various thermal conditions.
(K) Schematic of fiber-shaped TENG unit (top) and dye-sensitized solar cells (bottom).
(L) Demonstration of the hybridized power textile during outdoor activities on a human subject.
Reprinted with permission from: (A and B) Xu et al.[98] Copyright 2013, Springer Nature. (C and D) Park et al.[99] Copyright 2018, Springer Nature. (E and F) Bandodkar et al.[100] Copyright 2017, The Royal Society of Chemistry. (G and H) Wang et al.[101] Copyright 2016, Springer Nature. (I and J) Hong et al.[102] Copyright 2019, AAAS. (K and L) Wen et al.[103] Copyright 2016, AAAS.

Organic electrochemical transistors were demonstrated as cardiac sensors, which could be attached to skin and biological tissues for cardiac signal recording.

Biofuel Cells

The unique skin interface of wearable sensors has inspired research of energy harvesting directly from the human body. Utilizing human biofluids such as sweat is an appealing approach, since biofuels including lactate and glucose are abundant in sweat and can be oxidized using enzymes. As shown in Figure 10E, a sweat lactate-based flexible biofuel cell (BFC) array composed of 3D CNT bioanode and cathode in a serpentine island-bridge configuration was designed.[100] The anodes and cathodes were arranged in an interdigitated format, with a Au island-bridge structure to hold the same neighboring electrodes (i.e., anode-anode, cathode-cathode) together and polyimide serpentine bridges to hold opposite electrodes together. This design enabled uniform distribution of stress around the disc

electrodes and prevented short-circuits between opposite electrodes. Lactate oxidase (LOx) enzyme was drop-cast on the 3D porous carbon nanotube-naphthoquinone (CNT-NQ) anodes, while cathodes were composed of compact carbon nanotube-silver oxide (CNT-Ag_2O) structures. When lactate is present in sweat, oxidation of lactate at the anode and reduction of Ag_2O to Ag at the cathode will occur. The wearable BFC exhibited stable performance under repeated strains of 50% and an impressive power density of nearly 1.2 mW cm^{-2} at 0.2 V, which was sufficient to power conventional electronics such as LEDs and a low-power Bluetooth radio while worn on skin (Figure 10F).

Triboelectric Nanogenerator and Piezoelectric Nanogenerator

Triboelectric generators operate by electrical potential of static polarized charges through mechanically agitated separation, which converts mechanical energy to electricity.[104] For example, a TENG device was woven into a coat and shoes that enabled continuous powering of wearable electronics only by human motion (Figures 10G and 10H).[101] The tube-shaped TENG tube guaranteed stable performance under multiple directions of mechanical motion, which could drive an electronic watch and fitness tracker during walking or jogging. Similar to TENGs described above, piezoelectric generators harvest energy from body motion. An interesting demonstration was shown to incorporate both tactile sensing and energy-harvesting schemes together in a PDMS-based e-skin.[105] Thin films of SWCNTs served as top/bottom electrodes and porous and UV ozone (UVO)-treated PDMS and air gap served as dielectric layers. Various mechanical stimuli such as pressure, bending, and stretching were differentiated based on changes in capacitance and film resistance with high sensitivity and fast response/recovery time. The air gaps and charges on UVO-treated porous PDMS were utilized to generate voltage and current, and at low pressure range (<1 kPa) the change in voltage generated was linearly dependent on the pressure applied and the change in air gap. The power-conversion efficiency was estimated to be ca. 8%, higher than theoretical conversion efficiency of nanowire-based piezoelectric nanogenerators. However, the power density of piezoelectrics is strongly affected by the intensity of physical movements, and thus need to be combined with another power supply such as batteries for long-term operation.

Thermoelectrics

Thermal energy is another interesting power source utilizing body heat. Thermoelectric generators are based on the Seebeck effect, which converts heat from temperature difference using high Seebeck coefficient materials including Bi_2Te_3 and Sb_2Te_3. Recently, the first flexible and wearable thermoelectric device with long-term and large active cooling feature was introduced (Figure 10I).[102] Rigid inorganic thermoelectric pillars and flexible electrode materials were sandwiched between stretchable elastomer (Ecoflex) to realize a power density up to 25.1 mW cm^{-2} when the human subject sat in a cold environment (Figure 10J).

Hybrid

To compensate their low power densities compared with conventional batteries, hybridized systems are operated to collect multiple power sources simultaneously.[106] As shown in Figure 10K, a self-powered textile combined dye-sensitized solar cells with TENG to achieve reasonable energy conversion.[103] When attached to clothes, the hybrid textile could not only harvest solar energy from ambient light but also collect mechanical energy from human motion (Figure 10L). The gathered energy was then stored in fiber-shaped supercapacitors, which could sustainably operate wearable electronics.

While significant progress has been made in power supplies and power management, power source remains a bottleneck for skin electronic systems. Current flexible energy storage and harvesters are insufficient for complex sensor systems and not stable enough for long-term operations, especially in terms of size and weight. With its superior power density, batteries still represent the most popular choice, but flexible batteries require safety caution when under mechanical deformation. Flexible energy harvesters, on the other hand, have great potential in self-powered wearable systems but require a stable energy source such as sunlight, body motion, or biofluids. Advances in both power-efficient designs and more powerful energy supplies are expected in the future.

Communication and Data Analysis

Near-Field Communication

NFC is an emerging technology that enables two electronic devices to establish communication by simply placing them close to each other. For example, NFC-enabled thermography was combined with colorimetric microfluidic sensors for chloride sensing (Figures 11A and 11B).[107] An on-board temperature sensor was integrated with an NFC chip so that real-time diagnosis of sweat loss and electrolyte concentration could be obtained. Notably, NFC transmission enables not only data transfer but also power transfer. A hybrid skin-interfaced system was recently introduced with functionalities of electrochemical, colorimetric, and volumetric analysis of sweat.[108] The battery-free system consists of a thin NFC electronic module along with a microfluidic network (Figure 11C). The system is initiated by placing an NFC-enabled portable device in proximity so that wireless, real-time data acquisition along with digital images for colorimetric analysis can be realized (Figure 11D).[108] Despite the light weight and low power consumption, NFC technology has a maximum delivery distance of about 4 inches (~10 cm) and also requires the antenna to be kept in a particular orientation along with a proximal power source placed near the subject, which limits the range of activity of the subject and is therefore not convenient for long-term use.

Bluetooth Low Energy

Bluetooth low energy (BLE) provides an alternative communication platform for wearable healthcare. Compared with NFC, BLE has a faster transmission rate and a much larger readout distance of over 30 feet (~9 m), which is suitable for multifunctional sensing and durable wearing. In a typical design of an electrochemical sensor system, integrated devices consisting of a rechargeable battery, a microcontroller, signal-processing circuits, and Bluetooth transceiver were assembled on an FPCB board and connected to a flexible electrochemical sensor.[53] The Bluetooth collects real-time data, transmits to the user's cell phone, and finally uploads data to cloud servers (Figures 11E and 11F). However, the mechanical stiffness of a rigid BLE module is unfavorable for skin interfaces, and most commercially available BLE modules consume power on the order of milliwatts, which confers demanding power requirements.

Radiofrequency

Radiofrequency (RF) transmission operates at a fixed frequency of 13.56 MHz and obtains coupling between an initiator and a passive target. Figure 11G highlights a representative demonstration of a chip-free and battery-free on-skin sensor network that is wirelessly connected with flexible readout circuits attached to textiles through RF identification technology.[109] The stretchable sensors were composed of intrinsically soft materials without any rigid silicon circuits or batteries to ensure conformal skin interface, while the initiator circuit contained a Bluetooth transceiver

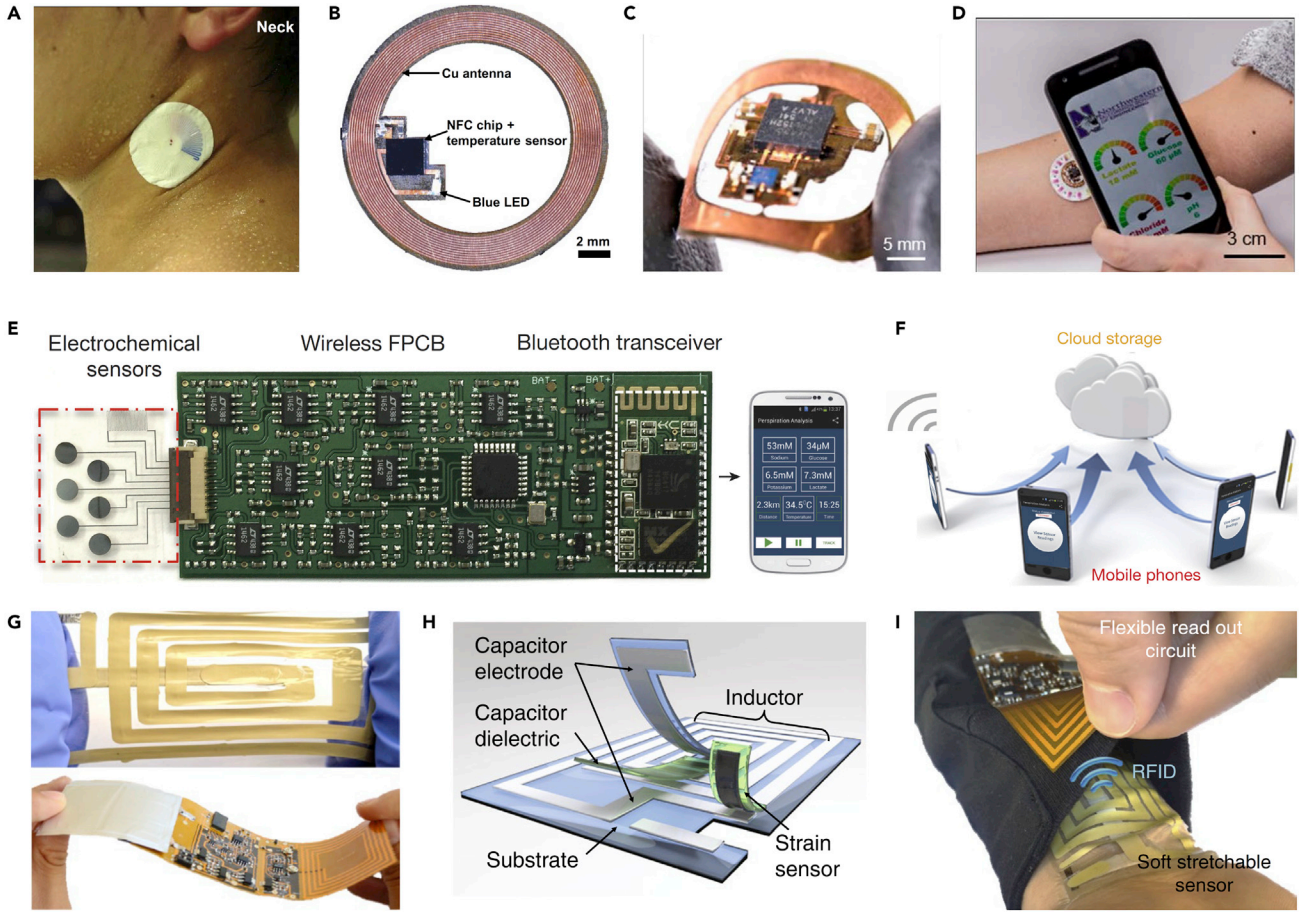

Figure 11. Communication and Data Analysis

(A) Photograph of sweat collection at the neck of a subject under high levels of deformation.
(B) Structure of NFC electronics for digital thermography and chloride sensing.
(C) Image of a battery-free NFC electronic sensor patch.
(D) Illustration of a phone interface for wireless communication and image acquisition.
(E) Image of a Bluetooth-enabled wearable platform with electrochemical sensors connected to a flexible PCB module.
(F) Demonstration of wireless sweat analysis by uploading data to cloud servers.
(G) Image of a wireless sensor network composed of stretchable on-skin sensors and flexible PCB initiator.
(H) Design of the stretchable sensor target node.
(I) Demonstration of pulse monitoring through a sensor node placed on a subject's wrist.
Reprinted with permission from: (A and B) Reeder et al.[107] Copyright 2019, AAAS. (C and D) Bandodkar et al.[108] Copyright 2019, AAAS. (E and F) Gao et al.[53] Copyright 2016, Springer Nature. (G–I) Niu et al.[109] Copyright 2019, Springer Nature.

for data communication to a smartphone (Figures 11H and 11I). The system was demonstrated to monitor pulse, breath, and body movement continuously.

The development of wireless communication and data analysis has enabled further miniaturization and integration of wearable sensor systems, although some limitations still need to be solved. NFC and RF communication can be built as fully flexible and conformal to the skin, but have a relatively short working distance and require an antenna-readout circuitry placed near the sensors. BLE can be transferred further and faster, but requires specialized integrated circuit chips and cannot be built flexibly at present. These wireless communication modules usually take a large fraction of power consumption, and thus need to

be combined with power management in order to develop a fully integrated sensor platform.[110]

CONCLUSION AND OUTLOOK

Skin-interfaced sensors hold great promise for future medical healthcare, especially with its non-invasive or minimally invasive sampling techniques and its compliance with human skin. In this review, we have outlined the material selection, structure design, and integration form factors that are pivotal to achieving soft and conformal skin-interfaced sensors. A list of key skin-interfaced physical, vital, and chemical sensors was further summarized based on different sensing targets, with emphases on design and performance of the sensor and interface. The significant advances in the field have set the foundation and attracted increased research interest. However, several factors still hamper the practical implementation of skin-interfaced sensors, such as stable and reliable operation in non-ideal conditions, sensitive detection and physiological correlations of more vital biomarkers, and sustainable and flexible power supply for prolonged system operation and wireless communication. Here, we present some prospective directions:

(1) Reliable sensitivity and stability under non-ideal conditions over long-term use. Many skin-interfaced sensors (either physical or chemical) exhibit excellent performance when the wearer is static and when external noise level is negligible, but fail to exhibit stable and reliable readings due to environmental noise or human motion artifacts. It is also useful to investigate the impact resistance of the sensors and the interface/encapsulation strategies so that a durable platform can be developed for daily wear and tear. In addition to external artifacts, chemical sensors can be especially susceptible to fouling events from the sampled biofluids, which could further damage the sensor performance and reliability over time. Insights from skin biology would be helpful for evaluating different measures to eliminate or reduce biofouling sources, and regeneration of chemical sensors would be a desirable feature for long-term use.

(2) Expansion of detection targets and correlation with gold-standard detection. Most of the current detection targets are limited to vital signs (e.g., temperature, ECG) and a few high-concentration molecular analytes (e.g., glucose, lactate, electrolytes). To augment the capability of skin-interfaced electronics, a broad spectrum of biomarkers of high medical impact should be investigated. Highly sensitive sensors and smart sensing strategies are necessary to measure the amounts of ultralow-level analytes and extract trends of some patterns shielded or hidden by different layers of epidermis or tissues. In addition to inventing functional sensors, it is also important to validate the sensor readings with gold-standard measurements to ensure that matrix effect/external interference is resolved. The clinical impact of such biomarkers should also be evaluated by investigating the relationship/correlation between serum and sweat/ISF biomarkers, with the potential influences from sweat rate. Understanding the secretion mechanism of such biomarkers would be beneficial to sensor design and application.

(3) Enhanced computational approaches and data analyses for personalized monitoring and disease prediction/prognosis. As more sensors are developed and multimodal sensing is integrated into one device, smart data storage and analyses become an essential task. Data pre-treatment with smart filtering will aid in understanding sensing results, and machine learning could be applied to help clinicians discover patterns related to disease

prediction and prognosis. It will be particularly useful if multimodal sensing data could be combined for characterization, augmenting the accuracy/precision of the data-based decision. Personal medicine could be realized as treatment is adjusted in a more proactive manner based on the data analyses obtained.

(4) Miniaturization of devices and improvements in wearability and fabrication. The practical implementation of all skin-interfaced sensors faces the challenge of improving the user's wearability. The wearability could be improved by shrinking the size of the devices but, most importantly, skin biology should be taken into consideration to avoid irritation events over long-term use. This is especially applicable where electrical currents are applied to the skin and/or electronics are partially exposed to skin. Careful selection of thin materials that harbor breathability, stretchability, and no cytotoxicity will be helpful in improving the wearers' comfort. To enable a large-scale application of skin-interfaced sensors, scalable fabrication of skin-interfaced electronics is also necessary.

To date, a number of companies and startups are developing skin-interfaced wearable sensors, including L'ORÉAL's UV sensor for UV exposure detection, GE Healthcare's Novii wireless patch system for maternal/fetal heart rate monitoring, and MC10's BioStamp nPoint EMG sensor. Many wearable chemical sensors are also being commercialized, including Gatorade's GX Sweat Patch for hydration and nutrients monitoring and Eccrine Systems' sweat platform for medication monitoring. Many of the sensors have received Food and Drug Administration 510(k) clearance, and a number of them are also under clinical trials. Although many sensor systems are still based on rigid designs and suffer from noise during daily wear due to the loose connection with skin, these examples of commercial practice hold great promise for digital personalized medicine, and further commercialization of fully flexible and stretchable platforms is expected in the future.

The development of practical and efficient skin-interfaced sensors involves coordinating material, structure, and compliant form factors according to the target use, with the aim of maximizing the sensitivity, stability, mechanical flexibility, and usability of the system. To realize the ideal skin-interfaced platform, interdisciplinary collaboration is needed to merge the knowledge and skills from fields such as chemistry, physics, engineering, and physiology. With the critical problems in skin-interfaced electronics addressed, wearable healthcare could be further implemented with diverse functionalities, and the healthcare industry could expect a major revolution in personalized medicine.

ACKNOWLEDGMENTS

This work was supported by the Rothenberg Innovation Initiative (RI^2) program at California Institute of Technology (Caltech), Caltech – City of Hope Biomedical Research Initiative, the Amgen Chem-Bio-Engineering Award, and National Institutes of Health grant 5R21NR018271.

AUTHOR CONTRIBUTIONS

Conceptualization, W.G.; Investigation, C.X.; Writing – Original Draft, C.X. and Y.Y.; Writing – Review & Editing, C.X., Y.Y., and W.G.; Supervision, W.G.

REFERENCES

1. Ray, T.R., Choi, J., Bandodkar, A.J., Krishnan, S., Gutruf, P., Tian, L., Ghaffari, R., and Rogers, J.A. (2019). Bio-integrated wearable systems: a comprehensive review. Chem. Rev. *119*, 5461–5533.
2. Wang, C., Wang, C., Huang, Z., and Xu, S. (2018). Materials and structures toward soft electronics. Adv. Mater. *30*, 1801368.
3. Someya, T., Bao, Z., and Malliaras, G.G. (2016). The rise of plastic bioelectronics. Nature *540*, 379–385.
4. Kim, J., Campbell, A.S., de Ávila, B.E.-F., and Wang, J. (2019). Wearable biosensors for healthcare monitoring. Nat. Biotechnol. *37*, 389–406.
5. Yang, Y., and Gao, W. (2019). Wearable and flexible electronics for continuous molecular monitoring. Chem. Soc. Rev. *48*, 1465–1491.
6. Choi, S., Lee, H., Ghaffari, R., Hyeon, T., and Kim, D.-H. (2016). Recent advances in flexible and stretchable bio-electronic devices integrated with nanomaterials. Adv. Mater. *28*, 4203–4218.
7. Rogers, J.A., Someya, T., and Huang, Y. (2010). Materials and mechanics for stretchable electronics. Science *327*, 1603–1607.
8. Rim, Y.S., Bae, S.-H., Chen, H., Marco, N.D., and Yang, Y. (2016). Recent progress in materials and devices toward printable and flexible sensors. Adv. Mater. *28*, 4415–4440.
9. Choi, S., Han, S.I., Kim, D., Hyeon, T., and Kim, D.-H. (2019). High-performance stretchable conductive nanocomposites: materials, processes, and device applications. Chem. Soc. Rev. *48*, 1566–1595.
10. Matsuhisa, N., Chen, X., Bao, Z., and Someya, T. (2019). Materials and structural designs of stretchable conductors. Chem. Soc. Rev. *48*, 2946–2966.
11. Wongkaew, N., Simsek, M., Griesche, C., and Baeumner, A.J. (2019). Functional nanomaterials and nanostructures enhancing electrochemical biosensors and lab-on-a-chip performances: recent progress, applications, and future perspective. Chem. Rev. *119*, 120–194.
12. Ladd, C., So, J.-H., Muth, J., and Dickey, M.D. (2013). 3D printing of free standing liquid metal microstructures. Adv. Mater. *25*, 5081–5085.
13. Ota, H., Chen, K., Lin, Y., Kiriya, D., Shiraki, H., Yu, Z., Ha, T.-J., and Javey, A. (2014). Highly deformable liquid-state heterojunction sensors. Nat. Commun. *5*, 5032.
14. Liu, Y., Liu, J., Chen, S., Lei, T., Kim, Y., Niu, S., Wang, H., Wang, X., Foudeh, A.M., Tok, J.B.-H., et al. (2019). Soft and elastic hydrogel-based microelectronics for localized low-voltage neuromodulation. Nat. Biomed. Eng. *3*, 58–68.
15. Cao, Y., Morrissey, T.G., Acome, E., Allec, S.I., Wong, B.M., Keplinger, C., and Wang, C. (2017). A transparent, self-healing, highly stretchable ionic conductor. Adv. Mater. *29*, 1605099.
16. Wang, Y., Zhu, C., Pfattner, R., Yan, H., Jin, L., Chen, S., Molina-Lopez, F., Lissel, F., Liu, J., Rabiah, N.I., et al. (2017). A highly stretchable, transparent, and conductive polymer. Sci. Adv. *3*, e1602076.
17. Zhang, F., Zang, Y., Huang, D., Di, C., and Zhu, D. (2015). Flexible and self-powered temperature–pressure dual-parameter sensors using microstructure-frame-supported organic thermoelectric materials. Nat. Commun. *6*, 8356.
18. Matsuhisa, N., Inoue, D., Zalar, P., Jin, H., Matsuba, Y., Itoh, A., Yokota, T., Hashizume, D., and Someya, T. (2017). Printable elastic conductors by *in situ* formation of silver nanoparticles from silver flakes. Nat. Mater. *16*, 834–840.
19. Lipomi, D.J., Vosgueritchian, M., Tee, B.C.-K., Hellstrom, S.L., Lee, J.A., Fox, C.H., and Bao, Z. (2011). Skin-like pressure and strain sensors based on transparent elastic films of carbon nanotubes. Nat. Nanotechnol. *6*, 788–792.
20. Yang, C., and Suo, Z. (2018). Hydrogel ionotronics. Nat. Rev. Mater. *3*, 125–142.
21. Annabi, N., Tamayol, A., Uquillas, J.A., Akbari, M., Bertassoni, L.E., Cha, C., Camci-Unal, G., Dokmeci, M.R., Peppas, N.A., and Khademhosseini, A. (2014). 25th anniversary article: rational design and applications of hydrogels in regenerative medicine. Adv. Mater. *26*, 85–124.
22. Sun, J.-Y., Zhao, X., Illeperuma, W.R.K., Chaudhuri, O., Oh, K.H., Mooney, D.J., Vlassak, J.J., and Suo, Z. (2012). Highly stretchable and tough hydrogels. Nature *489*, 133–136.
23. Sun, T.L., Kurokawa, T., Kuroda, S., Ihsan, A.B., Akasaki, T., Sato, K., Haque, M.A., Nakajima, T., and Gong, J.P. (2013). Physical hydrogels composed of polyampholytes demonstrate high toughness and viscoelasticity. Nat. Mater. *12*, 932–937.
24. Imran, A.B., Esaki, K., Gotoh, H., Seki, T., Ito, K., Sakai, Y., and Takeoka, Y. (2014). Extremely stretchable thermosensitive hydrogels by introducing slide-ring polyrotaxane cross-linkers and ionic groups into the polymer network. Nat. Commun. *5*, 1–8.
25. Yuk, H., Zhang, T., Lin, S., Parada, G.A., and Zhao, X. (2016). Tough bonding of hydrogels to diverse non-porous surfaces. Nat. Mater. *15*, 190–196.
26. Oh, J.Y., Rondeau-Gagné, S., Chiu, Y.-C., Chortos, A., Lissel, F., Wang, G.-J.N., Schroeder, B.C., Kurosawa, T., Lopez, J., Katsumata, T., et al. (2016). Intrinsically stretchable and healable semiconducting polymer for organic transistors. Nature *539*, 411–415.
27. Kang, J., Tok, J.B.-H., and Bao, Z. (2019). Self-healing soft electronics. Nat. Electron. *2*, 144–150.
28. Sekitani, T., Noguchi, Y., Hata, K., Fukushima, T., Aida, T., and Someya, T. (2008). A rubberlike stretchable active matrix using elastic conductors. Science *321*, 1468–1472.
29. Kim, H.-J., Sim, K., Thukral, A., and Yu, C. (2017). Rubbery electronics and sensors from intrinsically stretchable elastomeric composites of semiconductors and conductors. Sci. Adv. *3*, e1701114.
30. Shim, H., Sim, K., Ershad, F., Yang, P., Thukral, A., Rao, Z., Kim, H.-J., Liu, Y., Wang, X., Gu, G., et al. (2019). Stretchable elastic synaptic transistors for neurologically integrated soft engineering systems. Sci. Adv. *5*, eaax4961.
31. Zou, Z., Zhu, C., Li, Y., Lei, X., Zhang, W., and Xiao, J. (2018). Rehealable, fully recyclable, and malleable electronic skin enabled by dynamic covalent thermoset nanocomposite. Sci. Adv. *4*, eaaq0508.
32. Byun, S.-H., Sim, J.Y., Zhou, Z., Lee, J., Qazi, R., Walicki, M.C., Parker, K.E., Haney, M.P., Choi, S.H., Shon, A., et al. (2019). Mechanically transformative electronics, sensors, and implantable devices. Sci. Adv. *5*, eaay0418.
33. Zhao, Y., Xing, G., and Chai, Z. (2008). Are carbon nanotubes safe? Nat. Nanotechnol. *3*, 191–192.
34. Maynard, A.D. (2016). Are we ready for spray-on carbon nanotubes? Nat. Nanotechnol. *11*, 490–491.
35. Kaltenbrunner, M., Sekitani, T., Reeder, J., Yokota, T., Kuribara, K., Tokuhara, T., Drack, M., Schwödiauer, R., Graz, I., Bauer-Gogonea, S., et al. (2013). An ultra-lightweight design for imperceptible plastic electronics. Nature *499*, 458–463.
36. Sekitani, T., Yokota, T., Zschieschang, U., Klauk, H., Bauer, S., Takeuchi, K., Takamiya, M., Sakurai, T., and Someya, T. (2009). Organic nonvolatile memory transistors for flexible sensor arrays. Science *326*, 1516–1519.
37. Kim, J., Gutruf, P., Chiarelli, A.M., Heo, S.Y., Cho, K., Xie, Z., Banks, A., Han, S., Jang, K.-I., Lee, J.W., et al. (2017). Miniaturized battery-free wireless systems for wearable pulse oximetry. Adv. Funct. Mater. *27*, 1604373.
38. Sun, Y., Choi, W.M., Jiang, H., Huang, Y.Y., and Rogers, J.A. (2006). Controlled buckling of semiconductor nanoribbons for stretchable electronics. Nat. Nanotechnol. *1*, 201–207.
39. Kim, D.-H., Ahn, J.-H., Choi, W.M., Kim, H.-S., Kim, T.-H., Song, J., Huang, Y.Y., Liu, Z., Lu, C., and Rogers, J.A. (2008). Stretchable and foldable silicon integrated circuits. Science *320*, 507–511.
40. Song, Z., Ma, T., Tang, R., Cheng, Q., Wang, X., Krishnaraju, D., Panat, R., Chan, C.K., Yu, H., and Jiang, H. (2014). Origami lithium-ion batteries. Nat. Commun. *5*, 3140.
41. Fan, J.A., Yeo, W.-H., Su, Y., Hattori, Y., Lee, W., Jung, S.-Y., Zhang, Y., Liu, Z., Cheng, H., Falgout, L., et al. (2014). Fractal design concepts for stretchable electronics. Nat. Commun. *5*, 3266.
42. Jang, K.-I., Li, K., Chung, H.U., Xu, S., Jung, H.N., Yang, Y., Kwak, J.W., Jung, H.H., Song, J., Yang, C., et al. (2017). Self-assembled three dimensional network designs for soft electronics. Nat. Commun. *8*, 15894.

43. Xu, S., Zhang, Y., Jia, L., Mathewson, K.E., Jang, K.-I., Kim, J., Fu, H., Huang, X., Chava, P., Wang, R., et al. (2014). Soft microfluidic assemblies of sensors, circuits, and radios for the skin. Science *344*, 70–74.

44. Someya, T., Kato, Y., Sekitani, T., Iba, S., Noguchi, Y., Murase, Y., Kawaguchi, H., and Sakurai, T. (2005). Conformable, flexible, large-area networks of pressure and thermal sensors with organic transistor active matrixes. Proc. Natl. Acad. Sci. U S A *102*, 12321–12325.

45. Lanzara, G., Salowitz, N., Guo, Z., and Chang, F.-K. (2010). A spider-web-like highly expandable sensor network for multifunctional materials. Adv. Mater. *22*, 4643–4648.

46. Choi, S., Han, S.I., Jung, D., Hwang, H.J., Lim, C., Bae, S., Park, O.K., Tschabrunn, C.M., Lee, M., Bae, S.Y., et al. (2018). Highly conductive, stretchable and biocompatible Ag-Au core-sheath nanowire composite for wearable and implantable bioelectronics. Nat. Nanotechnol. *13*, 1048–1056.

47. Khang, D.-Y., Jiang, H., Huang, Y., and Rogers, J.A. (2006). A stretchable form of single-crystal silicon for high-performance electronics on rubber substrates. Science *311*, 208–212.

48. Sim, K., Chen, S., Li, Z., Rao, Z., Liu, J., Lu, Y., Jang, S., Ershad, F., Chen, J., Xiao, J., et al. (2019). Three-dimensional curvy electronics created using conformal additive stamp printing. Nat. Electron. *2*, 471–479.

49. Kim, D.-H., Lu, N., Ma, R., Kim, Y.-S., Kim, R.-H., Wang, S., Wu, J., Won, S.M., Tao, H., Islam, A., et al. (2011). Epidermal electronics. Science *333*, 838–843.

50. Jia, W., Bandodkar, A.J., Valdés-Ramírez, G., Windmiller, J.R., Yang, Z., Ramírez, J., Chan, G., and Wang, J. (2013). Electrochemical tattoo biosensors for real-time noninvasive lactate monitoring in human perspiration. Anal. Chem. *85*, 6553–6560.

51. Miyamoto, A., Lee, S., Cooray, N.F., Lee, S., Mori, M., Matsuhisa, N., Jin, H., Yoda, L., Yokota, T., Itoh, A., et al. (2017). Inflammation-free, gas-permeable, lightweight, stretchable on-skin electronics with nanomeshes. Nat. Nanotechnol. *12*, 907–913.

52. Schwartz, G., Tee, B.C.-K., Mei, J., Appleton, A.L., Kim, D.H., Wang, H., and Bao, Z. (2013). Flexible polymer transistors with high pressure sensitivity for application in electronic skin and health monitoring. Nat. Commun. *4*, 1859.

53. Gao, W., Emaminejad, S., Nyein, H.Y.Y., Challa, S., Chen, K., Peck, A., Fahad, H.M., Ota, H., Shiraki, H., Kiriya, D., et al. (2016). Fully integrated wearable sensor arrays for multiplexed *in situ* perspiration analysis. Nature *529*, 509–514.

54. Lipani, L., Dupont, B.G.R., Doungmene, F., Marken, F., Tyrrell, R.M., Guy, R.H., and Ilie, A. (2018). Non-invasive, transdermal, path-selective and specific glucose monitoring via a graphene-based platform. Nat. Nanotechnol. *13*, 504–511.

55. Tian, X., Lee, P.M., Tan, Y.J., Wu, T.L.Y., Yao, H., Zhang, M., Li, Z., Ng, K.A., Tee, B.C.K., and Ho, J.S. (2019). Wireless body sensor networks based on metamaterial textiles. Nat. Electron. *2*, 243–251.

56. Liu, M., Pu, X., Jiang, C., Liu, T., Huang, X., Chen, L., Du, C., Sun, J., Hu, W., and Wang, Z.L. (2017). Large-area all-textile pressure sensors for monitoring human motion and physiological signals. Adv. Mater. *29*, 1703700.

57. Jung, S., Lee, J., Hyeon, T., Lee, M., and Kim, D.-H. (2014). Fabric-based integrated energy devices for wearable activity monitors. Adv. Mater. *26*, 6329–6334.

58. Wang, S., Xu, J., Wang, W., Wang, G.-J.N., Rastak, R., Molina-Lopez, F., Chung, J.W., Niu, S., Feig, V.R., Lopez, J., et al. (2018). Skin electronics from scalable fabrication of an intrinsically stretchable transistor array. Nature *555*, 83–88.

59. Sugiyama, M., Uemura, T., Kondo, M., Akiyama, M., Namba, N., Yoshimoto, S., Noda, Y., Araki, T., and Sekitani, T. (2019). An ultraflexible organic differential amplifier for recording electrocardiograms. Nat. Electron. *2*, 351–360.

60. Yang, J.C., Mun, J., Kwon, S.Y., Park, S., Bao, Z., and Park, S. (2019). Electronic skin: recent progress and future prospects for skin-attachable devices for health monitoring, robotics, and prosthetics. Adv. Mater. *0*, 1904765.

61. Webb, R.C., Bonifas, A.P., Behnaz, A., Zhang, Y., Yu, K.J., Cheng, H., Shi, M., Bian, Z., Liu, Z., Kim, Y.-S., et al. (2013). Ultrathin conformal devices for precise and continuous thermal characterization of human skin. Nat. Mater. *12*, 938–944.

62. Ota, H., Chao, M., Gao, Y., Wu, E., Tai, L.-C., Chen, K., Matsuoka, Y., Iwai, K., Fahad, H.M., Gao, W., et al. (2017). 3D printed "earable" smart devices for real-time detection of core body temperature. ACS Sens. *2*, 990–997.

63. Gao, L., Zhang, Y., Malyarchuk, V., Jia, L., Jang, K.-I., Chad Webb, R., Fu, H., Shi, Y., Zhou, G., Shi, L., et al. (2014). Epidermal photonic devices for quantitative imaging of temperature and thermal transport characteristics of the skin. Nat. Commun. *5*, 4938.

64. Zhu, C., Chortos, A., Wang, Y., Pfattner, R., Lei, T., Hinckley, A.C., Pochorovski, I., Yan, X., To, J.W.-F., Oh, J.Y., et al. (2018). Stretchable temperature-sensing circuits with strain suppression based on carbon nanotube transistors. Nat. Electron. *1*, 183–190.

65. Khan, Y., Ostfeld, A.E., Lochner, C.M., Pierre, A., and Arias, A.C. (2016). Monitoring of vital signs with flexible and wearable medical devices. Adv. Mater. *28*, 4373–4395.

66. Yamada, T., Hayamizu, Y., Yamamoto, Y., Yomogida, Y., Izadi-Najafabadi, A., Futaba, D.N., and Hata, K. (2011). A stretchable carbon nanotube strain sensor for human-motion detection. Nat. Nanotechnol. *6*, 296–301.

67. Lee, S., Reuveny, A., Reeder, J., Lee, S., Jin, H., Liu, Q., Yokota, T., Sekitani, T., Isoyama, T., Abe, Y., et al. (2016). A transparent bending-insensitive pressure sensor. Nat. Nanotechnol. *11*, 472–478.

68. Wang, C., Hwang, D., Yu, Z., Takei, K., Park, J., Chen, T., Ma, B., and Javey, A. (2013). User-interactive electronic skin for instantaneous pressure visualization. Nat. Mater. *12*, 899–904.

69. Kim, J., Lee, M., Shim, H.J., Ghaffari, R., Cho, H.R., Son, D., Jung, Y.H., Soh, M., Choi, C., Jung, S., et al. (2014). Stretchable silicon nanoribbon electronics for skin prosthesis. Nat. Commun. *5*, 5747.

70. Pang, C., Lee, G.-Y., Kim, T., Kim, S.M., Kim, H.N., Ahn, S.-H., and Suh, K.-Y. (2012). A flexible and highly sensitive strain-gauge sensor using reversible interlocking of nanofibres. Nat. Mater. *11*, 795–801.

71. Wang, X., Gu, Y., Xiong, Z., Cui, Z., and Zhang, T. (2014). Silk-molded flexible, ultrasensitive, and highly stable electronic skin for monitoring human physiological signals. Adv. Mater. *26*, 1336–1342.

72. Pang, C., Koo, J.H., Nguyen, A., Caves, J.M., Kim, M.-G., Chortos, A., Kim, K., Wang, P.J., Tok, J.B.-H., and Bao, Z. (2015). Highly skin-conformal microhairy sensor for pulse signal amplification. Adv. Mater. *27*, 634–640.

73. Wang, C., Li, X., Hu, H., Zhang, L., Huang, Z., Lin, M., Zhang, Z., Yin, Z., Huang, B., Gong, H., et al. (2018). Monitoring of the central blood pressure waveform via a conformal ultrasonic device. Nat. Biomed. Eng. *2*, 687–695.

74. Yokota, T., Zalar, P., Kaltenbrunner, M., Jinno, H., Matsuhisa, N., Kitanosako, H., Tachibana, Y., Yukita, W., Koizumi, M., and Someya, T. (2016). Ultraflexible organic photonic skin. Sci. Adv. *2*, e1501856.

75. Liu, Y., Norton, J.J.S., Qazi, R., Zou, Z., Ammann, K.R., Liu, H., Yan, L., Tran, P.L., Jang, K.-I., Lee, J.W., et al. (2016). Epidermal mechano-acoustic sensing electronics for cardiovascular diagnostics and human-machine interfaces. Sci. Adv. *2*, e1601185.

76. Son, D., Kang, J., Vardoulis, O., Kim, Y., Matsuhisa, N., Oh, J.Y., To, J.W., Mun, J., Katsumata, T., Liu, Y., et al. (2018). An integrated self-healable electronic skin system fabricated via dynamic reconstruction of a nanostructured conducting network. Nat. Nanotechnol. *13*, 1057–1065.

77. Tian, L., Zimmerman, B., Akhtar, A., Yu, K.J., Moore, M., Wu, J., Larsen, R.J., Lee, J.W., Li, J., Liu, Y., et al. (2019). Large-area MRI-compatible epidermal electronic interfaces for prosthetic control and cognitive monitoring. Nat. Biomed. Eng. *3*, 194–205.

78. Kim, M.K., Kantarcigil, C., Kim, B., Baruah, R.K., Maity, S., Park, Y., Kim, K., Lee, S., Malandraki, J.B., Avlani, S., et al. (2019). Flexible submental sensor patch with remote monitoring controls for management of oropharyngeal swallowing disorders. Sci. Adv. *5*, eaay3210.

79. Jeong, J.-W., Kim, M.K., Cheng, H., Yeo, W.-H., Huang, X., Liu, Y., Zhang, Y., Huang, Y., and Rogers, J.A. (2014). Capacitive epidermal electronics for electrically safe, long-term electrophysiological measurements. Adv. Healthc. Mater. *3*, 642–648.

80. Ha, T., Tran, J., Liu, S., Jang, H., Jeong, H., Mitbander, R., Huh, H., Qiu, Y., Duong, J., Wang, R.L., et al. (2019). A chest-laminated

ultrathin and stretchable E-tattoo for the measurement of electrocardiogram, seismocardiogram, and cardiac time intervals. Adv. Sci. *6*, 1900290.

81. Mahmood, M., Mzurikwao, D., Kim, Y.-S., Lee, Y., Mishra, S., Herbert, R., Duarte, A., Ang, C.S., and Yeo, W.-H. (2019). Fully portable and wireless universal brain-machine interfaces enabled by flexible scalp electronics and deep learning algorithm. Nat. Mach. Intell. *1*, 412–422.

82. Yu, Y., Nyein, H.Y.Y., Gao, W., and Javey, A. (2019). Flexible electrochemical bioelectronics: the rise of in situ bioanalysis. Adv. Mater. *0*, 1902083.

83. Heikenfeld, J., Jajack, A., Feldman, B., Granger, S.W., Gaitonde, S., Begtrup, G., and Katchman, B.A. (2019). Accessing analytes in biofluids for peripheral biochemical monitoring. Nat. Biotechnol. *37*, 407–419.

84. Ghoneim, M.T., Nguyen, A., Dereje, N., Huang, J., Moore, G.C., Murzynowski, P.J., and Dagdeviren, C. (2019). Recent progress in electrochemical pH-sensing materials and configurations for biomedical applications. Chem. Rev. *119*, 5248–5297.

85. Bariya, M., Nyein, H.Y.Y., and Javey, A. (2018). Wearable sweat sensors. Nat. Electron. *1*, 160–171.

86. Yang, Y., Song, Y., Bo, X., Min, J., Pak, O.S., Zhu, L., Wang, M., Tu, J., Kogan, A., Zhang, H., et al. (2020). A laser-engraved wearable sensor for sensitive detection of uric acid and tyrosine in sweat. Nat. Biotechnol. *38*, 217–224.

87. Lee, H., Choi, T.K., Lee, Y.B., Cho, H.R., Ghaffari, R., Wang, L., Choi, H.J., Chung, T.D., Lu, N., Hyeon, T., et al. (2016). A graphene-based electrochemical device with thermoresponsive microneedles for diabetes monitoring and therapy. Nat. Nanotechnol. *11*, 566–572.

88. Kim, J., Jeerapan, I., Imani, S., Cho, T.N., Bandodkar, A., Cinti, S., Mercier, P.P., and Wang, J. (2016). Noninvasive alcohol monitoring using a wearable tattoo-based iontophoretic-biosensing system. ACS Sens. *1*, 1011–1019.

89. Hauke, A., Simmers, P., Ojha, Y.R., Cameron, B.D., Ballweg, R., Zhang, T., Twine, N., Brothers, M., Gomez, E., and Heikenfeld, J. (2018). Complete validation of a continuous and blood-correlated sweat biosensing device with integrated sweat stimulation. Lab Chip *18*, 3750–3759.

90. Koh, A., Kang, D., Xue, Y., Lee, S., Pielak, R.M., Kim, J., Hwang, T., Min, S., Banks, A., Bastien, P., et al. (2016). A soft, wearable microfluidic device for the capture, storage, and colorimetric sensing of sweat. Sci. Transl. Med. *8*, 366ra165.

91. Sekine, Y., Kim, S.B., Zhang, Y., Bandodkar, A.J., Xu, S., Choi, J., Irie, M., Ray, T.R., Kohli, P., Kozai, N., et al. (2018). A fluorometric skin-interfaced microfluidic device and smartphone imaging module for in situ quantitative analysis of sweat chemistry. Lab Chip *18*, 2178–2186.

92. Yu, H., Li, D., Roberts, R.C., Xu, K., and Tien, N.C. (2012). An interstitial fluid transdermal extraction system for continuous glucose monitoring. J. Microelectromech. Syst. *21*, 917–925.

93. Pu, Z., Wang, R., Xu, K., Li, D., and Yu, H. (2015). A flexible electrochemical sensor modified by graphene and AuNPs for continuous glucose monitoring. 14th IEEE Sensors Conference 10.1109/ICSENS.2015.7370301.

94. Bandodkar, A.J., Jia, W., Yardımcı, C., Wang, X., Ramirez, J., and Wang, J. (2015). Tattoo-based noninvasive glucose monitoring: a proof-of-concept study. Anal. Chem. *87*, 394–398.

95. Chen, Y., Lu, S., Zhang, S., Li, Y., Qu, Z., Chen, Y., Lu, B., Wang, X., and Feng, X. (2017). Skin-like biosensor system via electrochemical channels for noninvasive blood glucose monitoring. Sci. Adv. *3*, e1701629.

96. Kim, J., Sempionatto, J.R., Imani, S., Hartel, M.C., Barfidokht, A., Tang, G., Campbell, A.S., Mercier, P.P., and Wang, J. (2018). Simultaneous monitoring of sweat and interstitial fluid using a single wearable biosensor platform. Adv. Sci. *5*, 1800880.

97. Liu, W., Song, M.-S., Kong, B., and Cui, Y. (2017). Flexible and stretchable energy storage: recent advances and future perspectives. Adv. Mater. *29*, 1603436.

98. Xu, S., Zhang, Y., Cho, J., Lee, J., Huang, X., Jia, L., Fan, J.A., Su, Y., Su, J., Zhang, H., et al. (2013). Stretchable batteries with self-similar serpentine interconnects and integrated wireless recharging systems. Nat. Commun. *4*, 1543.

99. Park, S., Heo, S.W., Lee, W., Inoue, D., Jiang, Z., Yu, K., Jinno, H., Hashizume, D., Sekino, M., Yokota, T., et al. (2018). Self-powered ultra-flexible electronics via nano-grating-patterned organic photovoltaics. Nature *561*, 516–521.

100. Bandodkar, A.J., You, J.-M., Kim, N.-H., Gu, Y., Kumar, R., Mohan, A.M.V., Kurniawan, J., Imani, S., Nakagawa, T., Parish, B., et al. (2017). Soft, stretchable, high power density electronic skin-based biofuel cells for scavenging energy from human sweat. Energy Environ. Sci. *10*, 1581–1589.

101. Wang, J., Li, S., Yi, F., Zi, Y., Lin, J., Wang, X., Xu, Y., and Wang, Z.L. (2016). Sustainably powering wearable electronics solely by biomechanical energy. Nat. Commun. *7*, 1–8.

102. Hong, S., Gu, Y., Seo, J.K., Wang, J., Liu, P., Meng, Y.S., Xu, S., and Chen, R. (2019). Wearable thermoelectrics for personalized thermoregulation. Sci. Adv. *5*, eaaw0536.

103. Wen, Z., Yeh, M.-H., Guo, H., Wang, J., Zi, Y., Xu, W., Deng, J., Zhu, L., Wang, X., Hu, C., et al. (2016). Self-powered textile for wearable electronics by hybridizing fiber-shaped nanogenerators, solar cells, and supercapacitors. Sci. Adv. *2*, e1600097.

104. Wu, C., Wang, A.C., Ding, W., Guo, H., and Wang, Z.L. (2019). Triboelectric nanogenerator: a foundation of the energy for the new era. Adv. Energy Mater. *9*, 1802906.

105. Park, S., Kim, H., Vosgueritchian, M., Cheon, S., Kim, H., Koo, J.H., Kim, T.R., Lee, S., Schwartz, G., Chang, H., et al. (2014). Stretchable energy-harvesting tactile electronic skin capable of differentiating multiple mechanical stimuli modes. Adv. Mater. *26*, 7324–7332.

106. Chen, J., Huang, Y., Zhang, N., Zou, H., Liu, R., Tao, C., Fan, X., and Wang, Z.L. (2016). Micro-cable structured textile for simultaneously harvesting solar and mechanical energy. Nat. Energy *1*, 16138.

107. Reeder, J.T., Choi, J., Xue, Y., Gutruf, P., Hanson, J., Liu, M., Ray, T., Bandodkar, A.J., Avila, R., Xia, W., et al. (2019). Waterproof, electronics-enabled, epidermal microfluidic devices for sweat collection, biomarker analysis, and thermography in aquatic settings. Sci. Adv. *5*, eaau6356.

108. Bandodkar, A.J., Gutruf, P., Choi, J., Lee, K., Sekine, Y., Reeder, J.T., Jeang, W.J., Aranyosi, A.J., Lee, S.P., Model, J.B., et al. (2019). Battery-free, skin-interfaced microfluidic/electronic systems for simultaneous electrochemical, colorimetric, and volumetric analysis of sweat. Sci. Adv. *5*, eaav3294.

109. Niu, S., Matsuhisa, N., Beker, L., Li, J., Wang, S., Wang, J., Jiang, Y., Yan, X., Yun, Y., Burnett, W., et al. (2019). A wireless body area sensor network based on stretchable passive tags. Nat. Electron. *2*, 361–368.

110. Kim, J., Ghaffari, R., and Kim, D.-H. (2017). The quest for miniaturized soft bioelectronic devices. Nat. Biomed. Eng. *1*, 0049.